HELLENIC REPUBLIC
National and Kapodistrian University of Athens
EST. 1837

"ALEXANDER FLEMING"
Biomedical Sciences Research Center

International MSc
Molecular Biomedicine

Oligodendroglial exosomes as potential targets for synucleinopathies

DIMITRA DIONYSOPOULOU

Center of Clinical Research, Experimental Surgery and Translational Research, Biomedical Research Foundation of the Academy of Athens (BRFAA), 4 Soranou Efesiou Street, 11527 Athens, Greece

Three Member Evaluation Committee

XILOURI MARIA

STEFANIS LEONIDAS

POLITIS PANAGIOTIS

Title

Oligodendroglial exosomes as potential targets for synucleinopathies

Authors and Affiliations

Dimitra Dionysopoulou

Center of Clinical Research, Experimental Surgery and Translational Research, Biomedical Research Foundation of the Academy of Athens (BRFAA), 4 Soranou Efesiou Street, 11527 Athens, Greece

Abstract

Multiple system atrophy (MSA) is characterized by alpha-synuclein (αSyn) accumulation in glial cytoplasmic inclusions (GCIs) within oligodendrocytes. Under normal conditions, αSyn cannot be detected in mature oligodendrocytes, thus supporting the prevailing hypothesis that the protein enters oligodendrocytes from the extracellular space, following its release by neighboring neurons, the cells physiologically expressing the protein. This can occur partly via the secretion of exosomes that act as transporters to facilitate the transmission of αSyn-related pathology, at least in neurons. Exosomes are small vesicles suggested to play a major role in the intercellular communication through the transport of multilevel information and cell-to-cell spreading of toxic molecules. Herein, we aimed to illuminate the contribution of oligodendroglial-derived exosomes in the development and spread of αSyn pathology in MSA-like experimental models. In our experimental design, we performed a comprehensive biochemical analysis of exosomes isolated from control OLN-93 rat oligodendroglial cell lines or cells stably overexpressing human αSyn or TPPP/p25α. To recapitulate MSA-like pathology *in vitro*, we incubated OLN cells for 48hours and 8 days with human PD amplified brain-derived fibrils and both intracellular and exosome-related αSyn levels were assessed by western immunoblotting and confocal microscopy. Our results indicate that both αSyn and TPPP/p25α can be released via oligodendroglial exosomes. Notably, the overexpression of hαSyn or TPPP/p25α accelerates the release of exosome-related αSyn and the addition of PD-fibrils evoked the packaging of high molecular weight, possible aggregated, αSyn species within exosomes. In addition, higher amounts of PD fibrils led to the phosphorylation of αSyn at Ser129, a strong indicator of pathology, but only in hαSyn-overexpressing cells, highlighting the contribution of the intracellular αSyn protein load in disease development. This line of research is important in uncovering the contribution of oligodendroglial-derived exosomes in the pathogenesis of alpha-synucleinopathies in general and in pinpointing the factors that mediate cell-to-cell communication, which may represent potential therapeutic targets.

Highlights

- PD patient-derived fibrils induce the formation of pathological αSyn assemblies within oligodendrocytes, which incorporate the endogenous seeded protein.
- Phosphorylation of αSyn at Ser129 occurs only in OLN-AS7 cells when treated with relative high amounts of PD-derived fibrils (detected at both 48 hours and 8 days post-fibril addition), possibly indicating that this depends on intracellular αSyn protein load.
- Addition of human αSyn PD patient-derived fibrils accelerates the exosome-associated release of αSyn in all OLN cell lines and affects p25α levels and distribution in cells stably overexpressing the human p25α protein.

Keywords

α-Synuclein; exosomes; multiple system atrophy; neurons; oligodendrocytes; Parkinson's disease; tubulin polymerization-promoting protein

Introduction

Multiple system atrophy (MSA) is an adult-onset, typically sporadic, fatal neurodegenerative condition of undetermined etiology, marked by the progressive loss of the autonomic nervous system[1, 2]. The onset of cerebral ataxia and dysautonomia as well as the occurrence of Parkinsonian symptoms are the disease's clinical hallmarks. MSA, together with Parkinson's Disease (PD), and Dementia with Lewy Bodies (DLB) are collectively referred to as alpha-synucleinopathies, due to the abnormal deposition of the misfolded neuronal pre-synaptic protein alpha-synuclein (αSyn)[3-8]. In particular, in PD and DLB αSyn accumulates in the neuronal cell soma or neurites forming the Lewy bodies and Lewy neurites, respectively, [5, 9]whereas in MSA, the protein deposits primarily in the cytoplasm of oligodendrocytes, forming glial cytoplasmic inclusions (GCIs) [10-13] and less frequently in neurons, forming neuronal cytoplasmic inclusions[14-16].

GCIs, which are the histopathological hallmark of MSA, are fibrillar structures composed of various aggregated proteins, with αSyn and tubulin polymerization–promoting protein p25α (TPPP/p25α) having a profound role in disease pathogenesis [11, 13, 17]. A significant correlation between the density of GCIs and neuronal demise has been reported, highlighting that GCIs are closely related to the neurodegenerative processes characterizing MSA [18].MSA is considered a primary oligodendrogliopathy, following the observation that widespread myelin degeneration may be the initial event in patient's brain, implying that the pathogenesis of MSA is mainly regulated by oligodendroglial malfunction [4, 8, 19]. Supporting evidence shows that oligodendrocytes of MSA brains have an abnormal accumulation of p25α and are significantly bigger in cell size[20].p25α is an oligodendroglial-specific phosphoprotein, physiologically facilitating myelination and stabilizing microtubule network [21]. In normal human brains, it co-localizes with the myelin basic protein (MBP), but this co-localization is lost in MSA [20]. The contribution of p25α in disease pathogenesis has been also highlighted by *in vitro* studies. In particular, it has been suggested that there is a significant correlation between p25α and αSyn, and p25α strongly stimulates the aggregation of αSyn *in vitro*[22, 23]. Moreover, p25α overexpression has been shown to interfere with the autophagic degradation of αSyn by preventing the fusion of autophagosomes with lysosomes and to enhance the secretion of αSyn via exophagy[24]. And more recently, published data from the host laboratory have shown that upon addition of human αSyn Pre-Formed Fibrils (PFFs) in primary mouse oligodendrocytes, p25α is redistributed from the oligodendroglial processes to the cell body and accumulates with αSyn-positive inclusions, in cells overexpressing human αSyn[25].

αSyn is physiologically localized at pre-synaptic terminals of neuronal cells[26] and is tightly associated with synaptic vesicle membranes and SNARE complex assembly [27-30]. Mature oligodendrocytes are not considered to express αSyn physiologically[31], thus the origin of αSyn within oligodendrocytes of MSA patients still remains enigmatic. The two possible scenarios that have been proposed include that under pathological conditions, oligodendrocytes either overexpress αSyn or internalize neuronally-derived αSyn from their surrounding neurons[32-38]. In support to the first hypothesis, different groups have reported the expression of the *SNCA* mRNA, encoding for αSyn, in oligodendrocytes, indicating the presence of the endogenous protein within oligodendrocytes[31, 34, 39]. However, others were not able to detect oligodendroglial *SNCA* mRNA expression in the brains of MSA patients [40, 41], or when

detected, no differences were reported between healthy controls and MSA patients[32, 42]. Regarding the second hypothesis, accumulating evidence suggests that αSyn can be secreted from healthy neurons and can be found intracellularly [43, 44]. Neuronal cells can secrete different pathological conformations of αSyn, varying from soluble monomers to insoluble fibrillar forms, which then propagate in a "prion-like" manner, having detrimental effects on the recipient cells[45, 46].More specifically, following the prion-like hypothesis, misfolded neuronal-secreted αSyn could be taken up by neighboring oligodendrocytes, where it can template the seeding of the endogenous protein, promoting the endogenous αSyn misfolding. Gradually, large insoluble aggregates are formed and other proteins are also recruited, leading to the formation of GCIs[47]. In favor of this scenario, different studies have indeed shown that exogenous recombinant monomers and higher order αSyn species, as well as neuronally derived αSyn, can be internalized and accumulated by primary oligodendrocytes and immortalized oligodendroglial cell lines[25, 33-38, 48, 49]. This cell-to-cell transmission maybe partly mediated via extracellular vesicles, such as exosomes[50-53] and neuronally-secreted αSyn taken-up by oligodendrocytes could potentially underlie the pathogenic mechanisms in MSA.

Exosomes are small extracellular nanovesicles with a diameter of 30-150nm of endocytic origin. Their biogenesis results from the inward budding of the multivesicular bodies (MVBs) that leads to the progressive accumulation of intraluminal vesicles (ILVs) inside MVBs. These MVBs can then take two distinct routes: either fuse with lysosomes and degrade their content or fuse with the plasma membrane and release their ILVs in the extracellular space, as exosomes[54]. Exosomes can be found in different biological fluids, such as blood plasma and serum, breast milk, urine and cerebrospinal fluid (reviewed in [55]), and their cargo, which relates to the origin cell, involves proteins, RNAs and lipids that can be physiologically delivered to recipient cells[54, 56-61]. Different *in vitro* and *in vivo* studies have shown that neurons, oligodendrocytes, astrocytes, and microglia are able to secrete exosomes[62-65]. Physiologically, neuronal-derived exosomes play an important role in cell-to-cell communication through the secretion of their content to neighboring and distant cells, of both neuronal and glial origin[66-72], whereas glial-derived exosomes promote neuronal health [62, 73-75]. However, exosomes are considered to be able to shuttle pathological misfolded proteins in the brain, making them potential mediators of alpha-synucleinopathies (reviewed in [76]).Indeed, Emmanouilidou et al., proposed that secretion of αSyn is associated with membrane vesicles whose identity is compatible with exosomes, in a calcium-dependent manner in a WT αSyn–Tet-off inducible SH-SY5Y cell culture model [51]. In favor of this finding, another report showed that exosomes secreted from αSyn overexpressing SH-SY5Y mediates αSyn transmission between neuronal cells and in combination with lysosomal inhibition, higher levels of cellular αSyn content leading to an increase in exosomal- associated αSyn release and greater transmission of the protein between cells is observed, thus further highlighting that exosomal release may eventually influence αSyn protein load within cells [77]. Noteworthy, Danzer et al. reported that exosome-related αSyn oligomers show a higher capacity of being taken up by surrounding cells, as well as, having more toxic effects on recipient cells, compared to exosome-free forms of the protein in primary neurons and neuronal cells, uncovering a key mechanism in the spread of αSyn in the brain[52]. In accordance with previous observations, Grey et al. used a continuous Thioflavin T fluorescence assay to investigate αSyn aggregation, and found out that exosomes provide an environment that favors αSyn oligomerization process when mouse neuroblastoma cells (N2a) were treated with low concentrations of αSyn fibrils [78]. To further support this notion, they analyzed the molecular composition of released exosomes and showed that GM1 and GM2 ganglioside exosomal lipids are sufficient to accelerate the protein aggregation. *In vivo* experiments also suggest that misfolded and oligomeric αSyn seem to be rather associated with exosomes, thus supporting the scenario that pathological αSyn species can be spread via their interaction with membrane vesicles[79,

80]. Nevertheless, injecting extracellular vesicles into the striatum of wild-type mice seems to mediate the spread of human αSyn throughout the brain [81].

Collectively, exosomes are thought to be crucial mediators in the spread of pathology in alpha-Synucleinopathies serving as "Trojan horses" for the spread of pathological forms of αSyn aggregates between neurons and glial cells and for the promotion of neuroinflammation through the release of pro-inflammatory cytokines by activated glial cells, both of which may eventually result in neuronal demise. Exosomal research has drawn a lot of attention in the last decade mainly because of studies demonstrating its role in neuron-glia communication. Additionally, the ability to isolate brain exosomes from peripheral biological fluids suggests that exosomes may function as a potential window into patients' brains, allowing for the dynamic tracking of ongoing brain changes as the disease progresses. However, research regarding the relationship between exosomes and MSA onset and development, has been mostly limited to neuronal-derived exosomes. Herein, we seek to investigate the role of oligodendroglial-derived exosomes in the development and spread of pathology in MSA-like experimental models and examine the contribution of exosome-associated αSyn and p25α proteins in MSA pathogenesis. Towards this end, a comprehensive biochemical analysis of exosomes isolated from control immortalized rat oligodendroglial cells (OLN-93) or cells stably overexpressing human αSyn (OLN-AS7) or TPPP/p25α (OLN-p25α), was performed. To recapitulate the pathological conditions *in vitro*, we incubated the cells with human αSyn fibrils amplified from the brain of a PD patient. Our results indicate that both αSyn and p25α can be released via oligodendroglial-derived exosomes and the exosomal cargo of αSyn significantly increases compared to that of PBS-treated cells. Also, endogenous oligodendroglial αSyn, which under normal conditions exists in minuscule, non-detectable amounts, is recruited upon PD-derived fibril addition and is incorporated into pathology-related formations, thus playing a central role in the establishment of the MSA pathology. Noteworthy, intracellular pathology-related phosphorylation of αSyn in Ser129 highly depends on the intracellular αSyn protein load. Also, TPPP/p25α network collapses when PD-fibrils are added to the cells. This line of research is important in uncovering the contribution of oligodendroglial-derived exosomes in disease pathogenesis, which may represent potential therapeutic targets for alpha-synucleinopathies.

Methods and Materials

Cell culture of Oligodendroglial cell lines

Three different immortalized rat oligodendroglial (OLN) cell lines, provided by Dr Poul Henning Jensen (Aarhus University, Denmark), were used for this study: the immortalized control OLN-93 line, which was derived from primary Wistar rat brain glial cultures [82], and the OLN-AS7 and OLN-p25 lines, which were produced by transfecting the OLN-93 line with a pcDNA3.1 zeo(−) human α-Synuclein (hαSyn) or a pcDNA3.1 zeo(−) human p25α vector, respectively [83]. All cells were grown in Dulbecco's modified Eagle's medium (D6429; Gibco, Invitrogen, Carlsbad, CA, USA), supplemented with 10% Fetal Bovine Serum (10270; Gibco, Invitrogen, Carlsbad, CA, USA), 50 U/mL penicillin and 50 μg/mL streptomycin at 37 °C with 5% CO2 incubator. OLN-AS7 and OLN- p25α cells were maintained in 50 μg/mL Zeocin (R25001; Thermo Fisher Scientific, Waltham, MA, USA).

Preparation of α-synuclein fibrils amplified from PD-patients (PD fibrils)

PD patient-derived fibrils were produced by Dr Markus Zweckstetter (University of Göttingen, Germany),as previously described[84]. To amplify αSyn fibrils obtained from brain samples of two

distinct individuals whose pathology was verified with PD, the protein misfolding cyclic amplification (PMCA) technique was used (PD1 and PD2 fibrils). Details about the patients' demographics are presented in Table 1. Throughout the experiments, cells were treated with 1 or 6 μg/ml PD1 (patient #1), PD2 (patient #2), or PBS as a control for 48 hours or 8 days. Following treatment, the cells were either processed for immunocytochemistry and confocal microscopy or lysed and collected for western blot analysis, while their cultured medium was used for exosome isolation as described below. Most of the experiments included in this study were performed using the PD1 fibrils.

Negative Staining

Specimens were prepared by adsorbing 5-μL drops of fibrils onto 200 mesh formvar- carbon film-bearing grids (Electron Microscopy Sciences, Hatfield, PA, USA), rinsing with water and staining with a 2% w/w aqueous uranyl acetate solution for 2 min. The grids were examined in a Philips 420 transmission electron microscope at an acceleration voltage of 60 kV and photographed with a Megaview G2 CCD camera (Olympus SIS, Münster, Germany) and iTEM image capture software.

Proteinase-K digestion

Enzymatic digestion of PD patient-derived fibrils was performed using 3 μg/mL proteinase-K for 10 min at 37 °C. The enzymatic activity was stopped by adding 1% SDS, followed by incubation for 10 min at 65 °C. Samples were then processed for immunoblottingas described below.

Preparation of exosome-depleted cell culture medium

Exosome-depleted cell culture media was used to differentiate between serum (contained in the culture media)- and cell-derived exosomes[85]. In short, DMEM supplemented with 20% FBS and 1% penicillin/streptomycin was ultracentrifuged for at least 16 hours, at 100.000 x g at 4 C. The supernatant was collected, filtered using a 0.2 μm filter, and stored at 4°C. OLN-cells treated either with PD-derived fibrils or PBS, as a control, were cultivated in exosome-depleted cell culture medium diluted in DMEM containing only 1% penicillin/streptomycin (2% FBS), for 48 hours.

Cell-derived exosome purification

For the isolation of exosomes released in the culture media, OLN-cell lines were cultured in 150 mm dishes (Sarstedt, Cat. No. 83.3903) in DMEM containing 10% FBS and 1% penicillin/streptomycin. This medium was replaced with exosome-depleted media, 48 hours prior to exosome isolation, according to a previously published protocol by Théry et al. [85] Briefly, the exosome-depleted medium containing the secreted cell-derived exosomes, was collected and centrifuged at 400 × g for 10 min at 4°C to remove cellular debris. The supernatant was then ultracentrifuged at 100.000 × g for 2 hrs at 4°C and the exosome-enriched pellet was finally resuspended in 50 μl PBS and stored at -80°C, until further use.

Micro-Bradford assay

A standard curve of known bovine serum albumin (BSA) values was primarily created with a concentration range from 0 to 0.6 μg/μL, to assessthe total protein concentration in the exosomal samples. Then, 2 μl of each sample were sequentially added to a flat, transparent 96-well microplate (Greiner, Cat. No.: 655101) andincubated for 5 min at room temperature (in the dark) with 198μl of the

Bradford reagent. By measuring their absorbance at 595 nm in a microplate reader (Tecan) and plotting it against the BSA concentration, the total protein content of each samplewas estimated.

Acetyl-cholinesterase Enzyme (AchE) activity assay

The amount of exosomes was indirectly quantified by measuring the activity of acetylcholinesterase (AchE), an enzyme that is specifically enriched in these vesicles, as previously described [86]. A succession of AchE standards with concentration ranges between 0 and 0.64 ng/L were used to create a standard curve. After that, 10µL of each 5-fold diluted sample and 240 µL of the reaction mixture, which included 5,5'-dithiobis-[2-nitrobenzoic acid], acetylthiocholine, and PBS, was added to a flat transparent 96-well microplate in duplicate and incubated for 30 min at RT in the dark. To determine the AChE activity in the exosomal samples and assess the number of exosomes in our preparations, the optical density was measured at 405 nm, using a microplate reader (Tecan).

Subcellular fractionation

The cell pellets were homogenized in lysis buffers with progressively higher extraction strength, after being washed with PBS. All of the buffers contained protease (Roche, 11836170001) and phosphatase (Roche, 04406837001) inhibitors. Cells were first lysed with 1% Triton X-100-containing buffer (150 mMNaCl, 50 mMTris pH 7.6, 2 mM EDTA), placed on ice for 30 min, and then centrifuged at 13,000 g for 30 min at 4 °C. The supernatant was recovered to obtain the Triton-soluble fraction. After two PBS wash cycles, the pellet was resuspended in a solution containing 1% SDS (150 mMNaCl, 50 mMTris pH 7.6, 2 mM EDTA), sonicated (75 pulses at 40% power) , and centrifuged at 13,000 x g for 30 min to extract the SDS-soluble fraction. After two 5% SDS washes, the remaining pellet was finally solubilized in a solution containing 8 M urea and 5% SDS. After being heated for 30 min at 45°C and centrifuged at 13,000 x g for 30 min to generate the Urea-soluble fraction.

For the exosomal lysates, sonication (50 pulses at 20% power) was performed prior to immunoblot analysis.

Western immunoblotting

Samples of equal protein concentration were processed for protein electrophoresis in 12% SDS-PAGE gels in Tris–glycine buffer. The proteins were subsequently transferred onto nitrocellulose membranes and immunoblot analysis was performed using primary antibodies (Table 2a).Membranes were then probed with horseradish peroxidase-conjugated secondary antibodies, visualized with Clarity Max ECL Substrate (BIO-RAD), and exposed to Super RX film (Fuji Film). The immunoreactivity for each protein band intensity within the linear range of detection was quantified with ImageJ software. Differences in protein expression levels were estimated following normalization of all measurements by β-actin or alix as loading controls in case of total or exosomal protein levels, respectively. Between different primary antibody stainings, mild stripping was performed (Glycine 2M, NaCl 5M).

Trypsinization for exosomal surface proteins

To reduce any contamination of our exosomal preparations with alpha-synuclein fibrils loosely attached to exosomes,Trypsin (1 mg/ml) was added to exosomal samples (0.5 mg/ml) and the reaction was stopped by adding a protease inhibitor (4 mg/ml, Roche; 11836170001), as previously described

[87].Exosomes were again separated by centrifugation at 50.000 x g for 2 hours at 4°C and resuspended in PBS.

Lysosomal inhibition

For the lysosomal pathway inhibition, the general lysosomal inhibitor NH_4Cl was utilized. In particular, OLN-cells were cultivated in 150 mm dishes (Sarstedt, Cat. No. 83.3903) in DMEM containing 10% FBS and 1% penicillin/streptomycin. Cells were treated with PD-derived fibrils or PBS (as control) and exosome-depleted medium was added, 48 hours prior to cell collection and exosome isolation, NH_4Cl (0.02M) was added in exosome-depleted medium for 16 hours prior to cell and exosome collection. Cell pellets were collected and lysed and exosomes were isolated and processed for immunoblot analysis as above.

Immunocytochemistry (ICC) and confocal microscopy

For the immunofluorescence analysis, OLN cells were seeded in 24-well plates at a density of 15,000 cells/well (for analysis up to 48 hours) or 6,000 cells/well (for up to 8 days) on poly-D-lysine-coated(P7405; Sigma-Aldrich, St. Louis, MO, USA) coverslips. Following a 40-min fixation with 4% Paraformaldehyde (PFA), the cells were blocked in 10% normal goat serum with 0.4% Triton X-100 at room temperature for 1 hour prior to primary antibody addition (overnight incubation at 4 °C). Table 2a,b depicts the primary and fluorescent secondary antibodies utilized in the study. Antigen retrieval was performed for the detection of phosphorylated αSyn with the EP1536Y antibody, where coverslips were treated for 45 min with 0,05% Tween-20 in PBS that had been pre-heated to boiling point, prior to blocking. Cell nuclei were stained with the dye 4-,6-diamidine-2-phenylindole dihydrochloride (DAPI).Images were obtained using a Leica TCS SP5 confocal microscope combined with a dual (tandem) scanner. All confocal images were obtained under equivalent conditions of laser power, pinhole size and accumulation settings between the groups. ImageJ (v2.0.0) software was used to quantify relative protein levels expressed as area coverage (μm^2) or % area coverage, normalized to the total number of cells/field (the number of DAPI-stained nuclei).

Sonication of PD-derived αSyn fibrils

PD-derived αSyn fibrils were sonicated using a probe tip sonicator as described previously (Cho, Nodet et al. 2009). Briefly, PD-derived fibrils were sonicated with 60 pulses at 20% power, in sterile conditions. The cells were incubated with 6 μg/ml of PD-derived fibrils (pre- and post-sonication) or PBS as a control for either 48 hours or 8 days and processed for confocal microscopy, as described above.

Statistical analysis

All statistical analysis was performed utilizing GraphPad Prism 5. In particular, differences between or within groups were assessed by unpaired t-test, one-way analysis of variance (ANOVA) with Tukey's post hoc test and two-way ANOVA followed with Bonferroni's correction. Results are displayed as the mean ± standard error (SE), with a p value of < 0.05 considered as statistically significant. Results are based on the analysis of at least three independent experiments.

Table 1: Demographics of donor brain from PD patients

Disease Type	Age	Gender	Postmortem delay (hrs)	Cause of death	Disease duration (yrs)
PD1	79	Male	17	Acute myocardial infarction	7
PD2	82	Female	9	Pneumonia	8

Table 2a: Primary antibodies used either in western blotting (WB) or immunocytochemistry (ICC)

Primary Antibodies Against:	Clone	Cat. No.	Working dilutions		Species reactivity	Company
			WB	ICC		
Human αSyn	4B12	GTX21904	1:1000	-	mouse	Gene Tex
	LB-509	807701	-	1:1000	mouse	Biolegend
Total αSyn	D10	Sc-515879	-	1:500	mouse	Santa Cruz
	SYN-1	610787	1:1000	-	mouse	BD Transductions
Rodent αSyn	D37A6	4179	1:1000	1:400	rabbit	Cell Signaling
pSer129 αSyn	EP1536Y	ab51253	1:1000	1:100	rabbit	Abcam
Oxidized/Nitrated αSyn	SYN303	824301	-	1:1000	mouse	Biolegend
Aggregated αSyn	MJFR-14-6-4-2	ab209538	-	1:1000	rabbit	Abcam
p25α			1:1000	1:400	rabbit/ rat	Home-made

β-actin		TA309077	1:2000	-	mouse	OriGene
alix		2171	1:1000	-	mouse	Cell Signaling

Table 2b: Secondary antibodies and dyes used either in western blotting (WB) or immunocytochemistry (ICC)

Secondary Antibodies Against:	**Cat. No.**	**Working dilutions**		**Species reactivity**	**Company**
		WB	**ICC**		
Goat Anti-Mouse IgG-HRP conjugated	AP124P	1:5000	-	mouse	Sigma Aldrich
Goat Anti-Rabbit IgG-HRP conjugated	AP132P	1:2000	-	rabbit	Sigma Aldrich
CF555 red	20033	-	1:2000	rabbit	Biotium
	20030	-	1:2000	mouse	Biotium
	20096	-	1:2000	rat	Biotium
CF488A green	20012	-	1:2000	rabbit	Biotium
	20010	-	1:2000	mouse	Biotium
Cy5	115-175-146	-	1:500	mouse	Jackson Imm.
DAPI	10236276001	-	1:3000	-	Sigma Aldrich

Results

In vitro characterization of human αSyn fibrils amplified from the brains of PD patients

To assess whether any conformational differences between the fibrils amplified from the two different PD patients exist, we initially examined their structure by transmission electron microscopy. EM images revealed a distinct architecture between the two fibril types, with fibrils derived from the brain of patient 1 (PD1 fibrils) exhibiting a relative more elongated morphology compared to fibrils derived from the brain of patient 2 (PD2 fibrils), that have a more fragmented morphology (Fig.1a). Besides EM analysis, fibrils underwent proteolytic digestion with proteinase K (PK), to study potential differences in their digestion profiles. Following PK digestion, higher levels of αSyn species resistant to digestion were observed in PD2 fibrils, as compared to PD1 fibrils (Fig.1b). Finally, differences between the two different PD fibril types, became more evident when we examined their seeding capacity to template the endogenous rodent protein into the formation of potentially pathological species, when applied to rat oligodendroglial (OLN-93) cells. Comparison of the fluorescent signal obtained with antibodies specific for the human (LB-509) and the rodent (D37A6) αSyn revealed that the protein species engendered in OLN-93 cells inoculated with PD1 fibrils were more elongated, whereas those in PD2 fibril-treated cells appeared much shorter and fragmented(Fig.1c). This structural variability could be either due to an inherent heterogeneity of PD fibrils, related to the disparity of the demographic characteristics of the two PD-patients(Table 1), or may arose from the fibrilpreparation procedure. For the purposes of the current study we focused mostly on the effects attributed to PD1 fibrils, as described below.

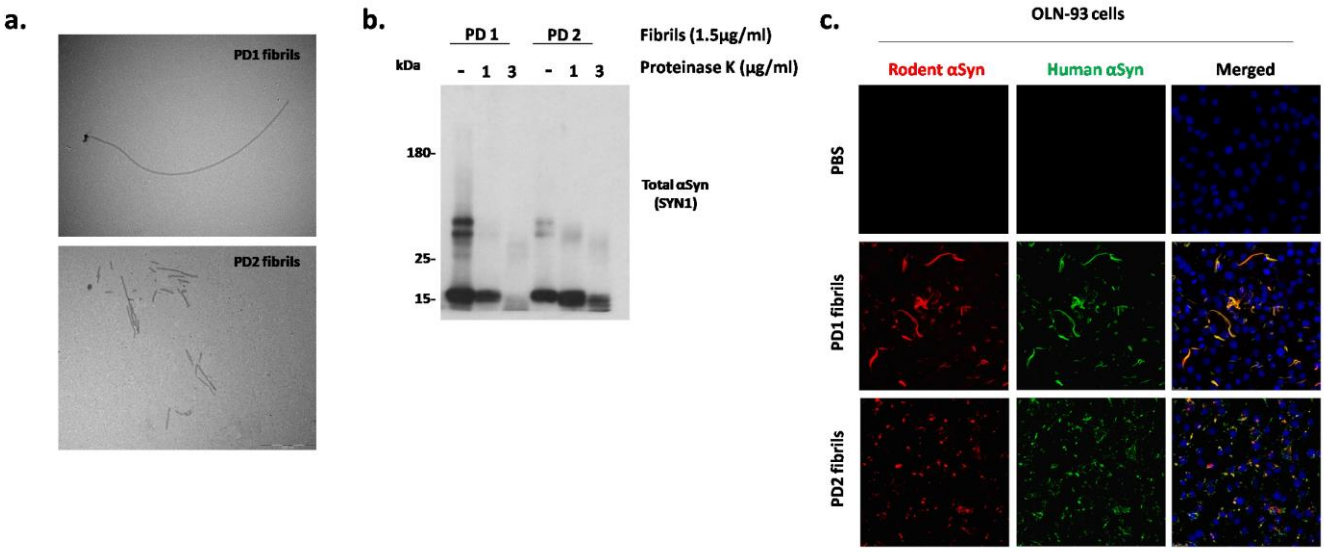

Figure 1 |*In vitro* characterization of human αSyn PD-derived fibrils. (1a) Representative transmission electron microscopy images of negatively stained PD1 (top) and PD2 (bottom) fibrils (Scale bar: 500nm).**(1b)**Western Immunoblotting analysis showing the Proteinase K (1and 3µg/ml)digestion profile of PD1 and PD2 fibrils (1.5µg/ml) using the SYN-1 antibody (recognizing both human and rodentαSyn). **(1c)**Representative immunofluorescence

images demonstrating the morphological differences of αSyn species formed in OLN-93 cell-lines treated with 1μg/ml of PD1 (middle) or PD2 (bottom) fibrils or PBS as control, first) for 48 hours using antibodies against human αSyn (green, LB-509) and endogenous rat αSyn (red, D37A6). DAPI staining is used as nuclear marker. Scale bar: 25μm.

PD1 patient-derived fibrils evoke the formation of Triton-insoluble αSyn assemblies intracellularly

To assess the ability of PD1 fibrils to act as a template for endogenous oligodendroglial αSyn to form insoluble protein species, we utilized the immortalized rat OLN-93 cell line that expresses very low to non-detectable levels of endogenous αSyn and p25α, as well as, the stable cell lines OLN-AS7 and OLN-p25α that overexpress the human αSyn or p25α, respectively. All OLN-cells were treated with 1μg/ml PD1 fibrils for 48 hours or 8 days and their cell pellet was sequentially fractionated using buffers with increasing extraction strength (Triton-, SDS- and Urea-containing buffers). As shown inFig.2a, Triton-solubleαSyn species were detected mostly in OLN-AS7 cells that run only as a monomer and did not differ between the PBS and the PD-1 fibril-treated cells. On the contrary, aberrant αSyn species were detected in SDS- and Urea- soluble fractions only in the fibril-treated cells (Fig.2a). In particular, truncated αSyn species were detected only in the SDS-soluble fraction, whereas high molecular weight (HMW) αSyn species were found in both SDS- and Urea-soluble fractions, possibly representing rather insoluble αSyn species. In both SDS- and Urea-soluble fractions, the peak levels of all αSyn conformations were detected at 48 hours that then declined following prolonged incubation in all lines(Fig.2b,c). Interestingly, in OLN-AS7 and OLN-p25α cells αSyn levels remained relatively higher as compared to OLN-93 control cells at 48 hours, thus highlighting the important role of αSyn and/or p25α intracellular protein load on the establishment of MSA-like pathology. The same trend was also observed following prolonged incubation (8 days) with PD1 fibrils, possibly indicating a relative resistance to degradation of αSyn species generated in the cells that overexpress human αSyn or p25α(Fig.2b,c).

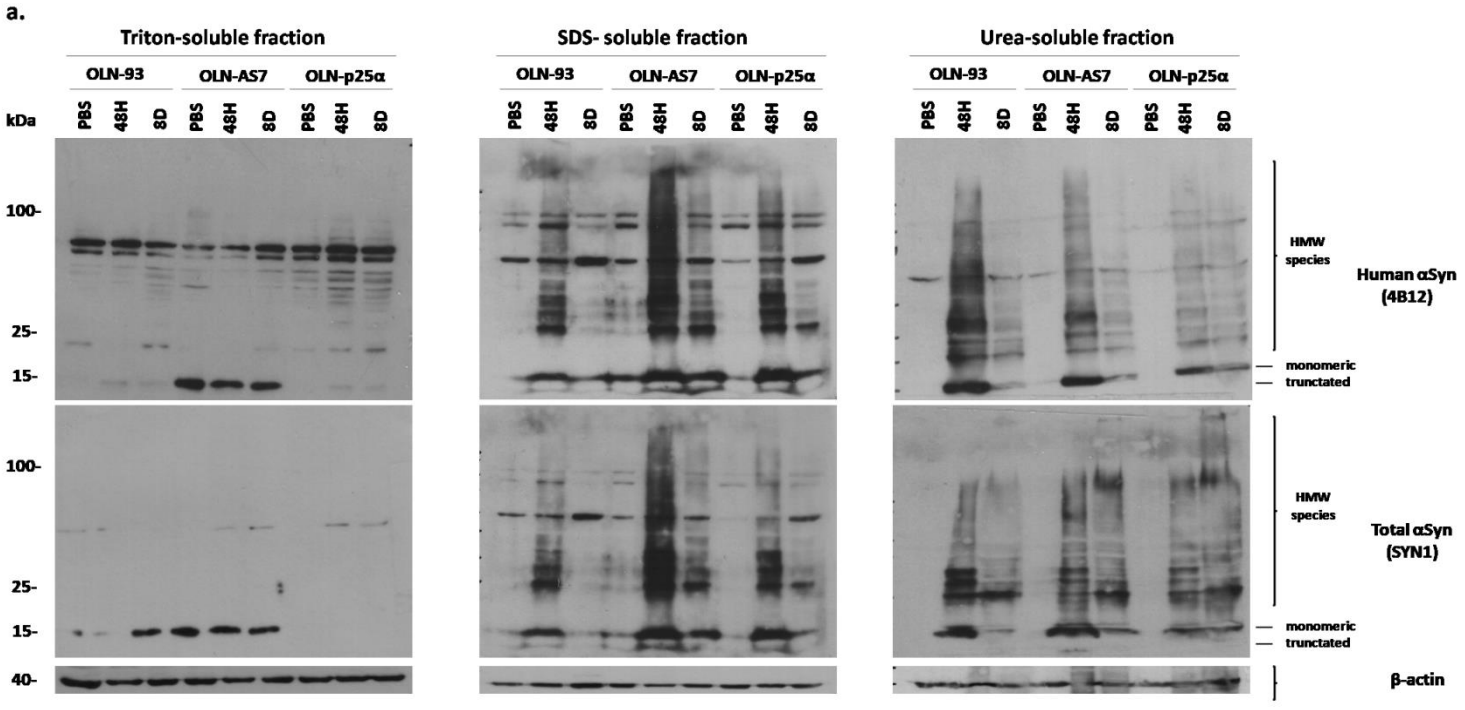

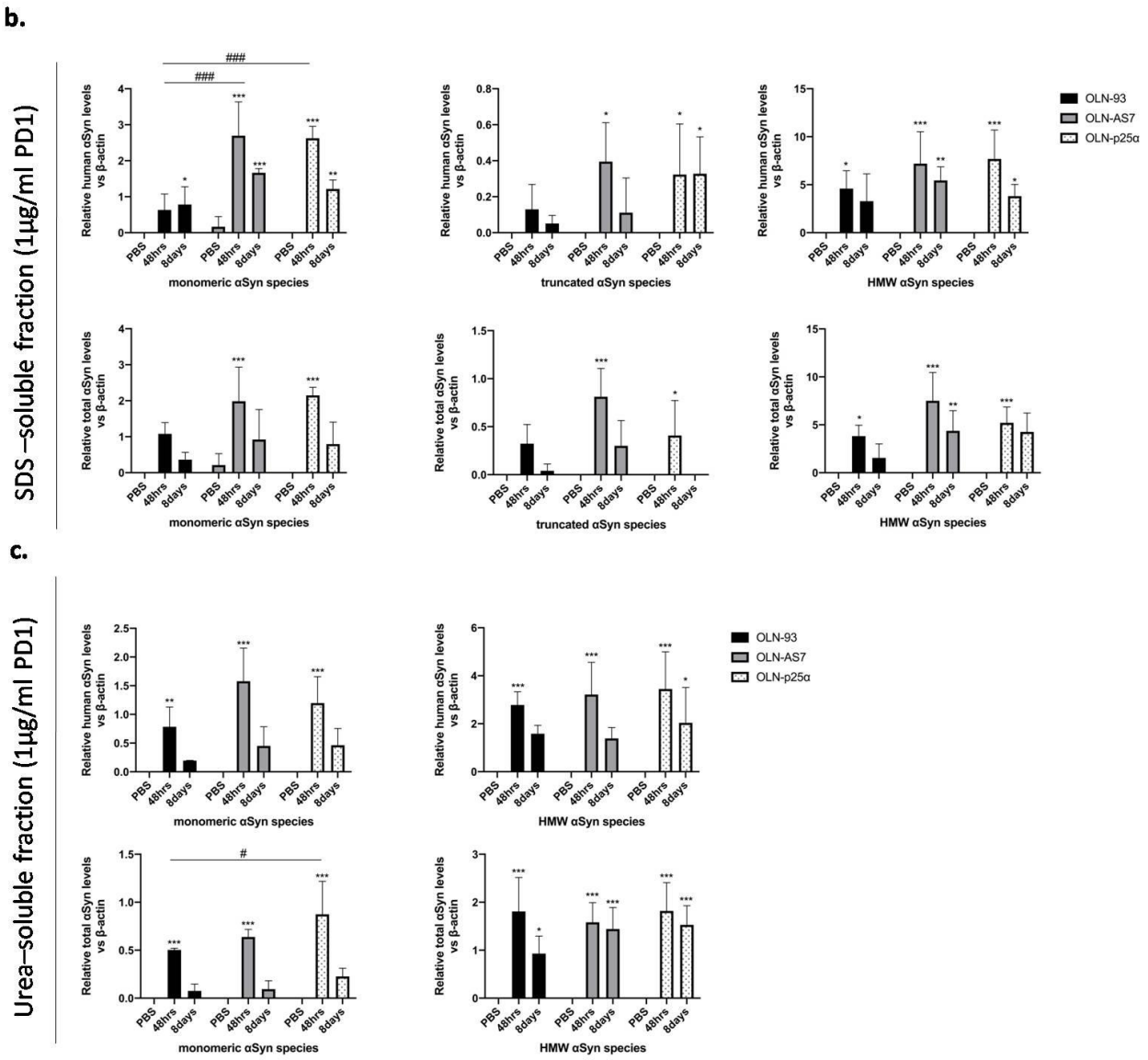

Figure 2 | Low concentrations of PD-patient derived fibrils evoke the formation of insoluble αSyn assemblies intracellularly. (2a) Representative immunoblots of the intracellular (Triton-, SDS-, UREA- soluble fraction)protein levels of human(4B12 antibody) and total (SYN-1 antibody) αSyn(monomeric, truncated and high-molecular weight species). All OLN cell lines were treated with 1 µg/ml PD1-amplified fibrils for either 48hours or 8days. **(2b,c)**Quantifications of the intracellular (SDS-, UREA- soluble fraction)protein levels of human(4B12 antibody) and total (SYN-1 antibody) αSyn(monomeric, truncated and high-molecular weight species). Equal loading is verified by the detection of β-actin (left). Data are expressed as the mean ± SD of at least three independent experiments; *p<0.05; **p<0.01; ***p<0.001, comparing PBS- and PD1 fibril-treated conditions within the same cell line and # p<0.05; ##p<0.01; #p<0.001, comparing between the different OLN-cell lines, by two-way ANOVA with Bonferroni's-correction.

PD1-patient derived fibrils recruit the endogenous rodent αSyn and evoke the formation of pathological αSyn species intracellularly

To investigate the ability of patient-derived fibrils to recruit the endogenous oligodendroglialαSyn, we used the rodent αSyn specific D37A6 antibody, in OLN-cells treated with 1μg/ml PD1 fibrils for 48 hours or 8 days. Indeed, PD1 fibrils evoke the recruitment of the endogenous rodent αSyn, whereas in the absence of fibrils (PBS), rodent αSyn is not detected (Fig. 3a).Noteworthy, this increased endogenous αSyn signal is co-localized with the exogenously added human αSyn patient derived material (LB-509)(Fig. 3a). Both rodent and human αSyn levels decrease over time in all OLN-cells, either due to the effective clearance of the formed αSyn species or to the dilution of exogenous human αSyn due to cell proliferation (Fig.3b). Interestingly, αSyn levels in OLN-AS7 cells at 48 hours were statistically significantly increased compared to control OLN-93 levels, further underlying the importance of the intracellular protein load of human αSyn on the seeding of pathology (Fig.3b). To further examine whether the endogenous rodent αSyn is incorporated into pathological αSyn assemblies following the addition of hαSyn PD fibrils, we assessed the formation of pathological αSyn species (Fig.4a). Specifically, we investigated the formation of oxidized/nitrated (SYN303) and aggregated (MJFR 14-6-4-2) αSyn species in all OLN-cells following treatment with 1μg/ml PD1 fibrils for either 48 hours or 8 days. Indeed, oxidized/nitrated αSyn was detected in all cells, with OLN-AS7 cells having statistically significant higher levels at 48 hours (Fig. 4b). More importantly, co-localization of SYN303 with the rodent αSyn (D37A6) antibody highlights the contribution of the endogenous OligodendroglialαSyn in the generation of pathology–related species within oligodendrocytes (Fig.4a). This conclusion was further supported by the complete co-localization of the conformation specific αSyn antibody (MJFR 14-6-4-2) with an antibody recognizing both the human and rodent αSyn (D10), suggesting that endogenous rodent αSyn is indeed a major component of the aggregated αSyn formations, as previously described [25] (Fig.4 a,b). Overall, the increased αSyn protein load of OLN-AS7 seems to contribute to the formation of pathological αSyn assemblies within oligodendrocytes to a greater extent as compared to the other OLN cells, which also incorporate the endogenous seeded protein.

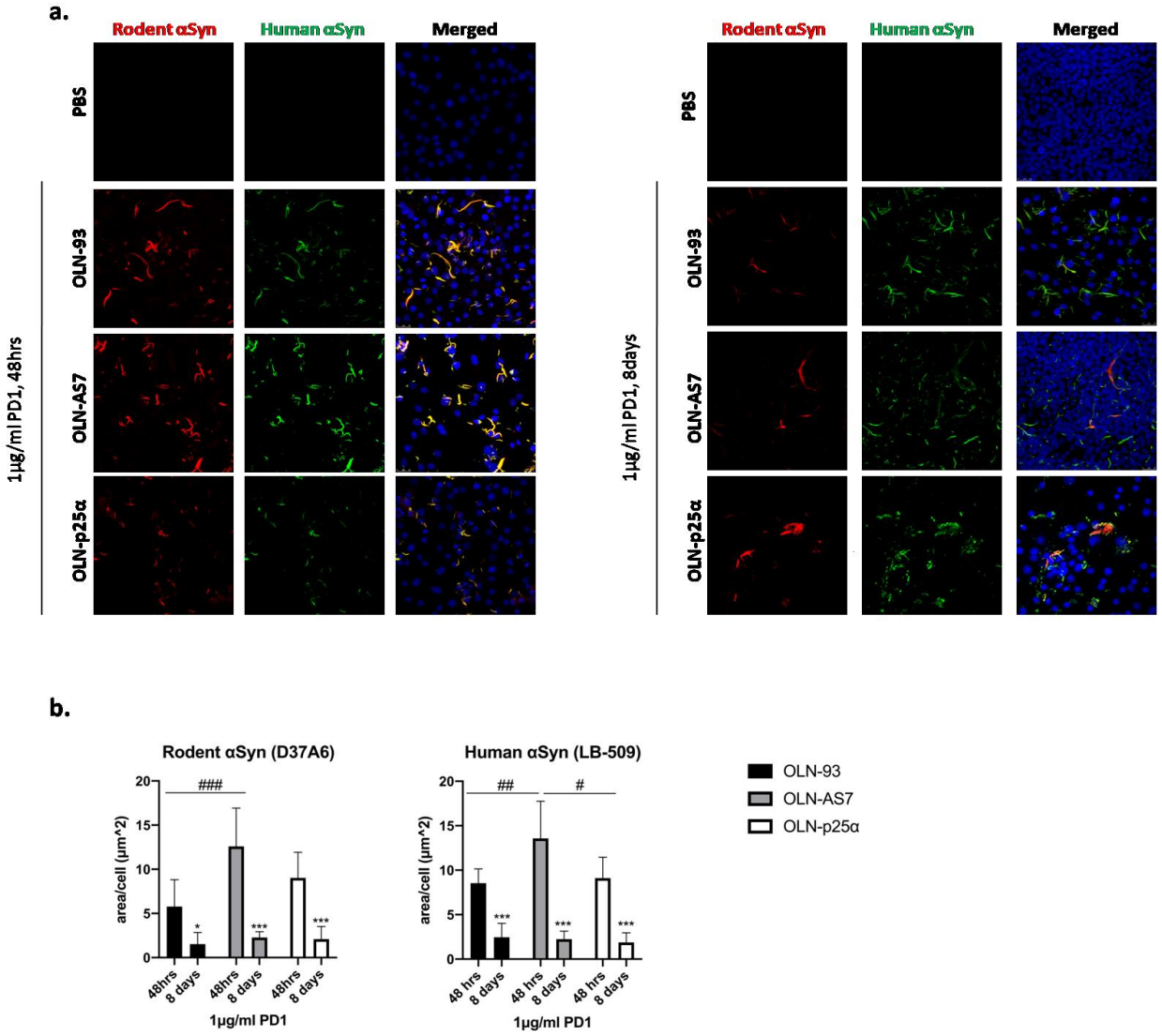

Figure 3 | Low concentrations of PD1-patient derived fibrils evoke the recruitment of the endogenous rodent αSyn. (3a) Representative immunofluorescence images using antibodies against human αSyn (**green**, LB-509) and endogenous rat αSyn (**red**, D37A6) in OLN- cell-lines treated with 1µg/ml of PD1 fibrils for 48 hours (left) or 8 days (right). DAPI staining is used as nuclear marker. Cells treated with PBS, in the absence of fibrils, were used as controls. Scale bar: 25µm.**(3b)** Quantifications of endogenous rat and human αSyn protein levels in OLN-cells expressed as area surface normalized to the total number of cells per image. Data are expressed as the mean ± SD of at least three independent experiments with triplicate samples/ condition within each experiment; *p<0.05; **p<0.01; ***p<0.001, comparing fibril-treated conditions within the same cell line and # p<0.05; ##p<0.01; #p<0.001, comparing between the different OLN-cell lines by two-way ANOVA with Bonferroni's-correction.

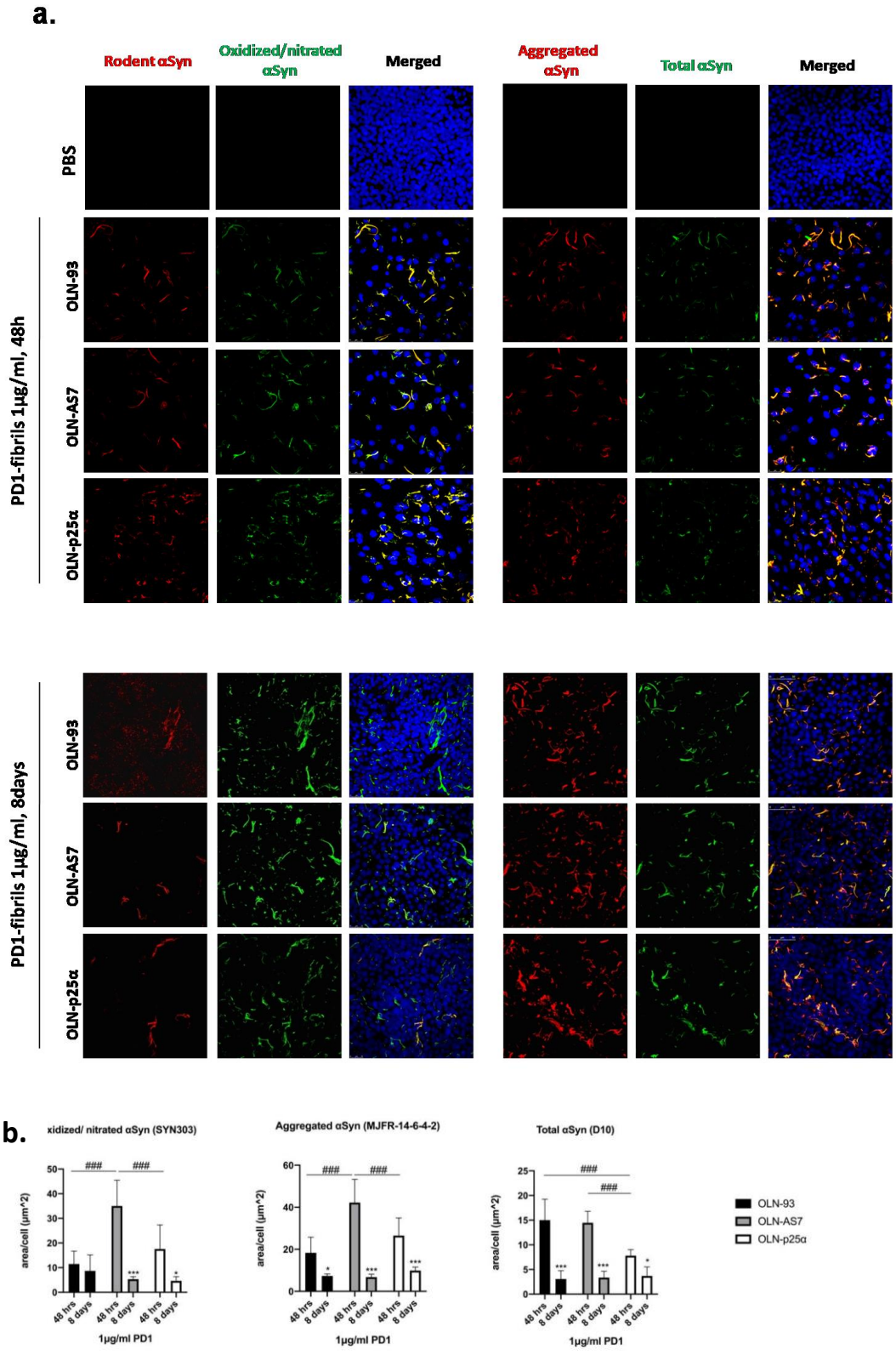
a.
Rodent αSyn
Oxidized/nitrated αSyn
Merged
Aggregated αSyn
Total αSyn
Merged
PBS
PD1-fibrils 1µg/ml, 48h
OLN-93
OLN-AS7
OLN-p25α
PD1-fibrils 1µg/ml, 8days
OLN-93
OLN-AS7
OLN-p25α
b.
xidized/ nitrated αSyn (SYN303)
Aggregated αSyn (MJFR-14-6-4-2)
Total αSyn (D10)
area/cell (µm^2)
48 hrs
8 days
1µg/ml PD1
OLN-93
OLN-AS7
OLN-p25α

Figure 4 | Low concentrations of PD1-patient derived fibrils evoke the formation of pathological αSyn species. (4a) Representative immunofluorescence images using antibodies against oxidized/nitrated αSyn (**green**, SYN303, first row), endogenous rodent αSyn (**red**, D37A6, second row), aggregated αSyn conformations (**red**, MJFR 14-6-4-2, forth row) and total αSyn (human and rodent, **green**, D10, fifth row) staining in OLN-cells treated with 1μg/ml of PD1 fibrils for 48 hours or 8 days. DAPI staining is used as nuclear marker. Scale bar: 25μm.**(4b)** Quantifications of oxidized/nitrated, aggregated and total αSyn protein levels in OLN-cells expressed as area surface normalized to the total number of cells per image. Data are expressed as the mean ± SD of at least three independent experiments with triplicate samples/condition within each experiment; *p<0.05; **p<0.01; ***p<0.001, comparing fibril-treated conditions within the same cell line and # p<0.05; ##p<0.01; #p<0.001, comparing between the different OLN-cell lines by two-way ANOVA with Bonferroni's-correction.

In vitro characterization of oligodendroglial-derived exosomes following treatment with human PD1-derived fibrils

Having established the formation of intracellular pathological αSyn species within oligodendrocytes following their inoculation with the PD-patient derived fibrils, we questioned whether such species may be also released extracellularly and may mediate the propagation of pathology. Our approach focused mostly on the contribution of exosomes, nanovesicles known to mediate αSyn release at least in neuronal cells[54]. To this end, oligodendroglial exosomes were isolated from the conditioned medium of OLN cells treated with PD1 fibrils (1 and 6 μg/ml for 48 hours or 8 days) and analyzed by EM and immunoblot analyses. EM images revealed the characteristic cup-shaped particles enclosed by a phospholipid bilayer enriched in our preparations(Fig. 5a) and immunoblot analysis verified the presence of αSyn and p25αprotein in exosomes isolated from the OLN-AS7 and OLN-p25α cells, respectively, under baseline conditions (data not shown). Using αSyn monomers of known concentrations run side-by-side with our exosomal-enriched preparations, we roughly estimated the quantity of monomeric human αSyn to be around 500nM, or even higher including the HMW species(Fig. 5b).In order to verify that the αSyn positive signal obtained in immunoblotting represents the protein species engendered within oligodendrocytes following treatment with the patient fibrils or reflects the human αSyn PD material added to the cell culture that was stuck in the outer exosomal membrane and sedimented with the exosomal pellet, we performed a series of control experiments. To this end, we initially run 2and 5 ng of PD1 fibrils together with exosomal extracts isolated from OLN-AS7 cells treated with either PBS (as control) or PD1 fibrils for 48 hours(Fig. 5c). The differential pattern of αSyn species obtained in the lanes where PD1 fibrils and exosomal samples were loaded, suggest that the protein detected in the exosomal preparations represents αSyn produced within the cells (Fig. 5c). In support of this notion, treatment of the exosomal preparations with trypsin to remove any residual contamination with PD1 fibrils loosely attached to exosomes revealed similar protein patterns between trypsinized and non-trypsinized samples, thus highlighting that the detected αSyn species are produced within PD1 fibril-treated OLN cells and released via exosomes(Fig. 5d).

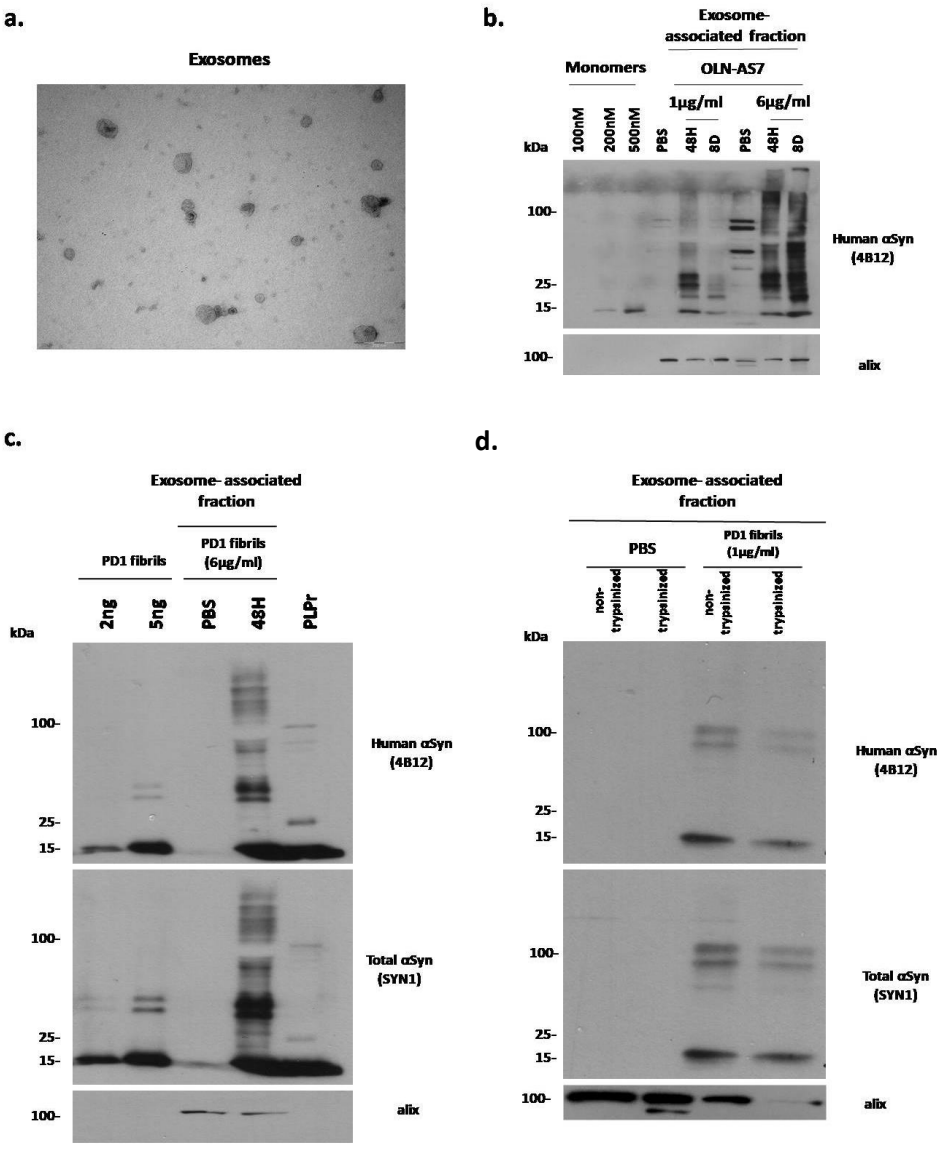

Figure 5 |*In vitro* characterization of oligodendroglial-derived exosomes following treatment with human αSyn PD-derived fibrils.(5a) Representative transmission electron microscopy images of negatively stained exosomes derived from PD1-treated OLN-cells. Scale bar: 200nm.**(5b)** Representative immunoblots against the human αSyn (4B12) of αSyn monomers (100, 200 and 500nM) and exosomal samples derived from OLN-cells treated with 1 or 6µg/ml PD1 fibrils for 48hours and 8days. **(5c)** Representative immunoblots against human (4B12) and total (SYN1) αSyn of PD1 fibrils (2 and 5ng) and exosomal samples derived from OLN-cells treated with 1µg/ml PD1 fibrils for 48hours. Brain lysate isolated from the PLP-hαSyn transgenic mice (MSA model) was used as a positive control for the detection of αSyn species. **(5d)** Representative immunoblots against human (4B12) and total (SYN1) αSyn of both trypsinized and non-trypsinized exosomal samples, derived from OLN-cells treated with 1µg/ml PD1 fibrils for 48h. Equal loading is verified by the detection of the exosomal marker alix.

Addition of PD1 patient derived fibrils enhances the exosome-associated release of αSyn

To examine the potential correlation between the cargo and the quantity of exosomes secreted from oligodendroglial cells treated with PD1 patient-amplified αSyn fibrils with the manifestation of αSyn pathology intracellularly, exosomes were isolated from the cell medium 48 hours and 8 days post fibril addition and were purified by ultracentrifugation. Following their isolation, immunoblot analysis was performed for the detection of human and total (human and rat) αSyn species (Fig. 6a).Interestingly, oligodendroglial exosomes were found to carry both monomeric and HMW αSyn (Fig. 6a,b), and rarely truncated αSyn species (data not shown). Quantitative analysis of the immunoblots revealed that the levels of human and total monomeric and HMW αSyn peak at 48 hours and then decrease over time in all OLN-cells. Importantly, in both OLN-AS7 and OLN-p25α cells αSyn protein levels released via exosomes were found to be significantly higher as compared to the control OLN-93 cell line, in agreement to the results obtained when the cell lysates were analyzed (Fig. 6b). Moreover, the quantity of exosomes derived from PD1-treated OLN-cells indirectly assessed by measuring the activity of acetylocholinesterase, an enzyme specifically enriched in these vesicles, revealed a trend for a decreased exosomal number at 48 hours, which was subsequently increased at 8 days, detected in all OLN-cells (Fig. 6c).

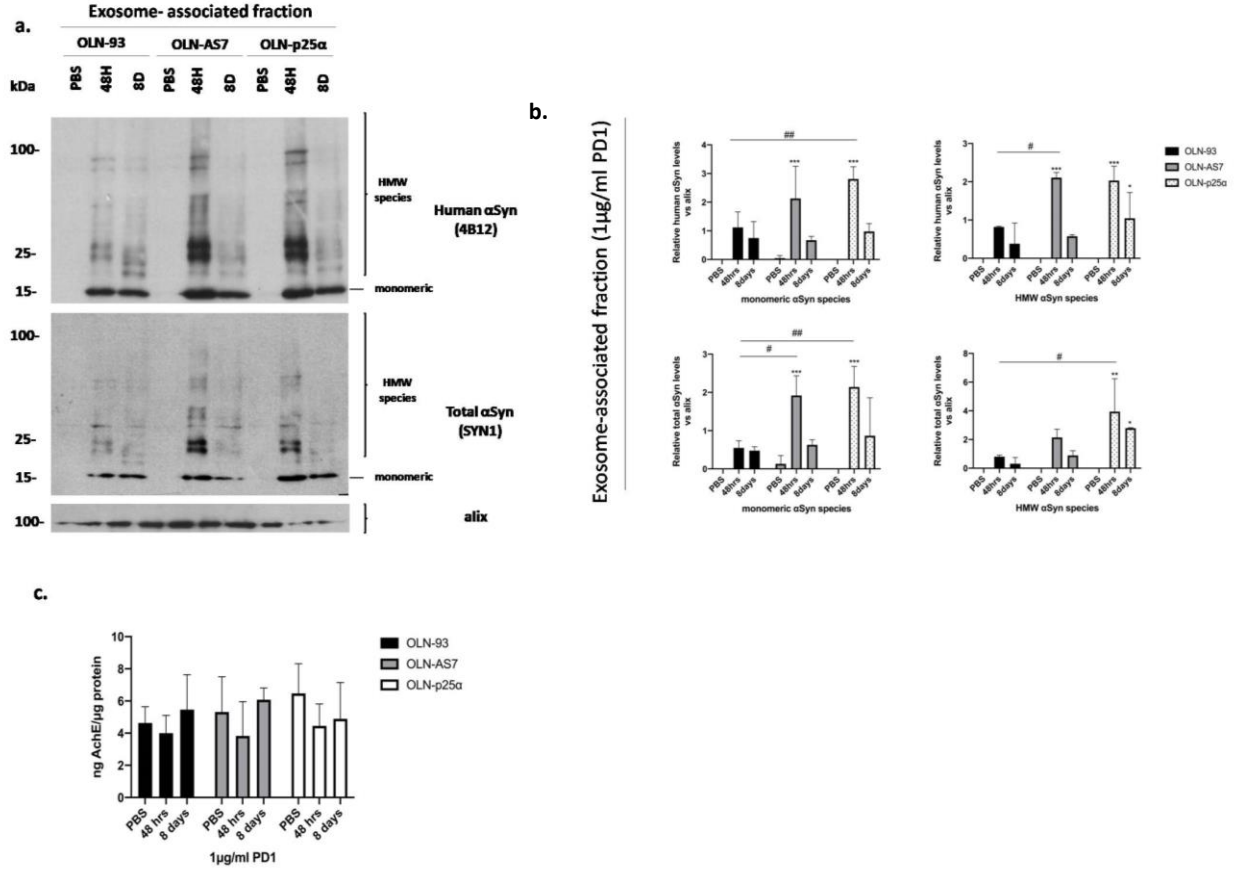

Figure 6 | Addition of low concentrations of human PD1 patient-derived fibrils enhances the exosome-associated release of αSyn. (6a) Representative immunoblots of the exosome-associated fractions demonstrating

the protein levels of human (4B12 antibody) and total (SYN-1 antibody) αSyn (monomeric and high-molecular weight species). All OLN cell lines were treated with 1 μg/ml PD1-amplified fibrils for either 48hours or 8days.**(6b)** Quantifications of the exosome-associated protein levels of human (4B12 antibody) and total (SYN-1 antibody) αSyn. Equal loading is verified by the detection of the exosomal marker alix. Data are expressed as the mean ± SD of at least three independent experiments; *p<0.05; **p<0.01; ***p<0.001, comparing PBS- and fibril-treated conditions within the same cell line and # p<0.05; ##p<0.01; #p<0.001, comparing between the different OLN-cell lines, by two-way ANOVA with Bonferroni's-correction **(6c)**Indirect quantification of the amount of the exosomal vesicles derived from PBS- and PD1 fibril- treated OLN-cells by measuring the activity of acetylocholinesterase enzyme normalized to the total protein load. Data are expressed as the mean ± SD of at least three independent experiments.

High concentrations of PD-patient derived fibrils evoke the formation of Triton-insoluble αSyn assemblies intracellularly

Given that the experiments using 1μg/ml PD1 fibrils pinpointed the significance of the total (endogenous and exogenously added) αSyn protein load present in OLN-cells for the formation of aberrant αSyn species (both intracellularly and extracellulary), we aimed to examine the effects of higher fibril concentrations in the seeding of pathology. To this end, OLN-AS7were incubated with 6μg/ml PD1 fibrils for 48 hours or 8 days, and cell pellets were again lysed using detergents of increased extraction strength (Triton-, SDS-, Urea- containing buffers). In contrast to what was observed in the lower fibril concentration (Fig.2a), monomeric as well as HMW αSyn species were detected in the Triton-soluble fraction at 48 hours post-fibril addition (Fig.7a).Similar findings were also observed in the SDS- and Urea-soluble fractions, were higher levels of monomeric and HMW αSyn protein species were detected in PD1 fibril-treated cells at 48 hours, that decreased over time(Fig. 7a,b).

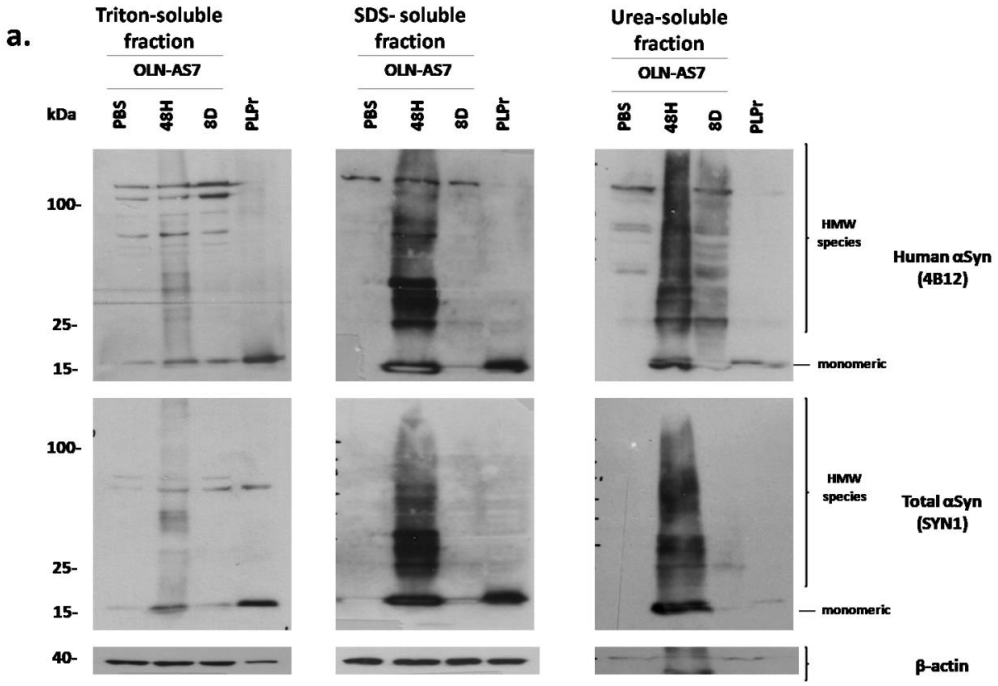

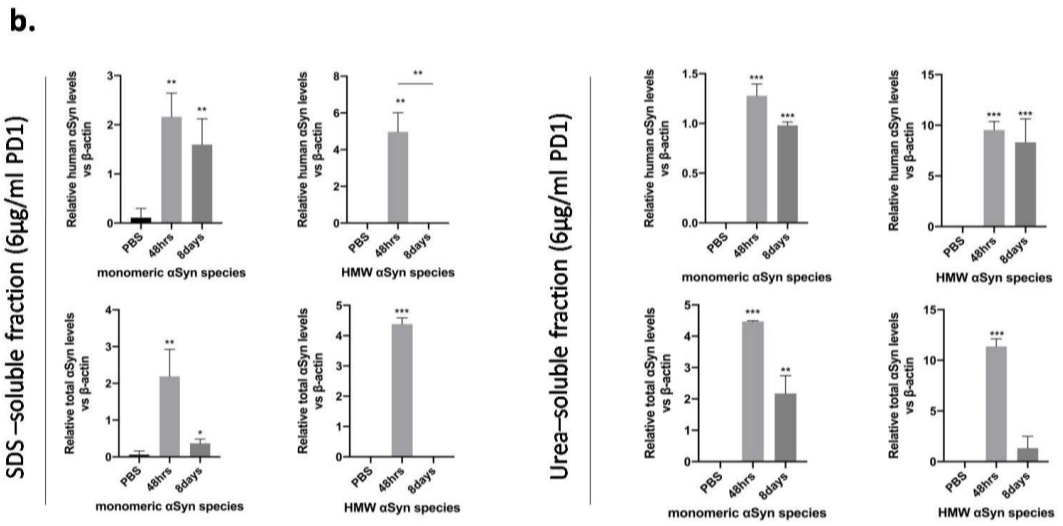

Figure 7 | High concentrations of PD-patient derived fibrils evoke the formation of Triton-insoluble αSyn assemblies intracellularly. (7a) Representative immunoblots of the intracellular (Triton-, SDS-, UREA- soluble fraction) protein levels of human(4B12 antibody) and total (SYN-1 antibody) αSyn (monomeric and high-molecular weight species).OLN-AS7 cells were treated with 6μg/ml PD1-amplified fibrils for either 48hours or 8days. Brain lysate isolated from the PLP-hαSyn transgenic mice (MSA model) was used as a positive control for the detection of αSyn species. **(7b)** Quantifications of the intracellular (SDS-, UREA- soluble fraction)protein levels of human(4B12 antibody) and total (SYN-1 antibody) αSyn (monomeric and high-molecular weight species). Equal loading is verified by the detection of β-actin. Data are expressed as the mean ± SD of at least three independent experiments; *p<0.05; **p<0.01; ***p<0.001, comparing PBS- and fibril-treated conditions within the same cell line by unpaired t-test.

High concentrations of PD-patient derived fibrils template the misfolding of the endogenous rodent αSyn into the formation of pathological αSyn species intracellularly

We then studied the ability of high concentrations of PD1 fibrils to also act as a template for the seeding of the endogenous rodent αSyn in oligodendroglial cells, expressed in miniscule amounts under basal conditions. Indeed, when PD1 fibrils were added to the cell medium, successful recruitment of the endogenous αSyn was detected, manifested by the robust increase of the fluorescent signal recognized by the rodent-specificαSyn antibody D37A6 (Fig. 8a). Once more, the peak levels were observed at 48 hours post-fibril addition in all OLN-cell lines, with OLN-AS7 and OLN-p25α reaching statistically significant higher levels than the control cell line, as previously reported using the lower fibril concentration of 1μg/ml (Fig. 8b). In addition, both oxidized/nitrated and aggregated forms of αSyn were again detected within the cytoplasm of all OLN cells treated with 6 μg/ml PD1 fibrils that followed a similar pattern with the rodent αSyn – peak at 48 hours and then drop at 8 days. However, oxidized/nitrated αSyn was particularly persistent following prolonged fibril incubation, in all OLN-cell lines (Fig.

9a,b). Aggregated αSyn was significantly higher at 48 hours in both OLN-AS7 and OLN-p25α cells, possibly indicating again the importance of the total intracellular protein load, either of αSyn or p25α, respectively, for the formation ofαSyn pathology within oligodendrocytes (Fig. 9b).

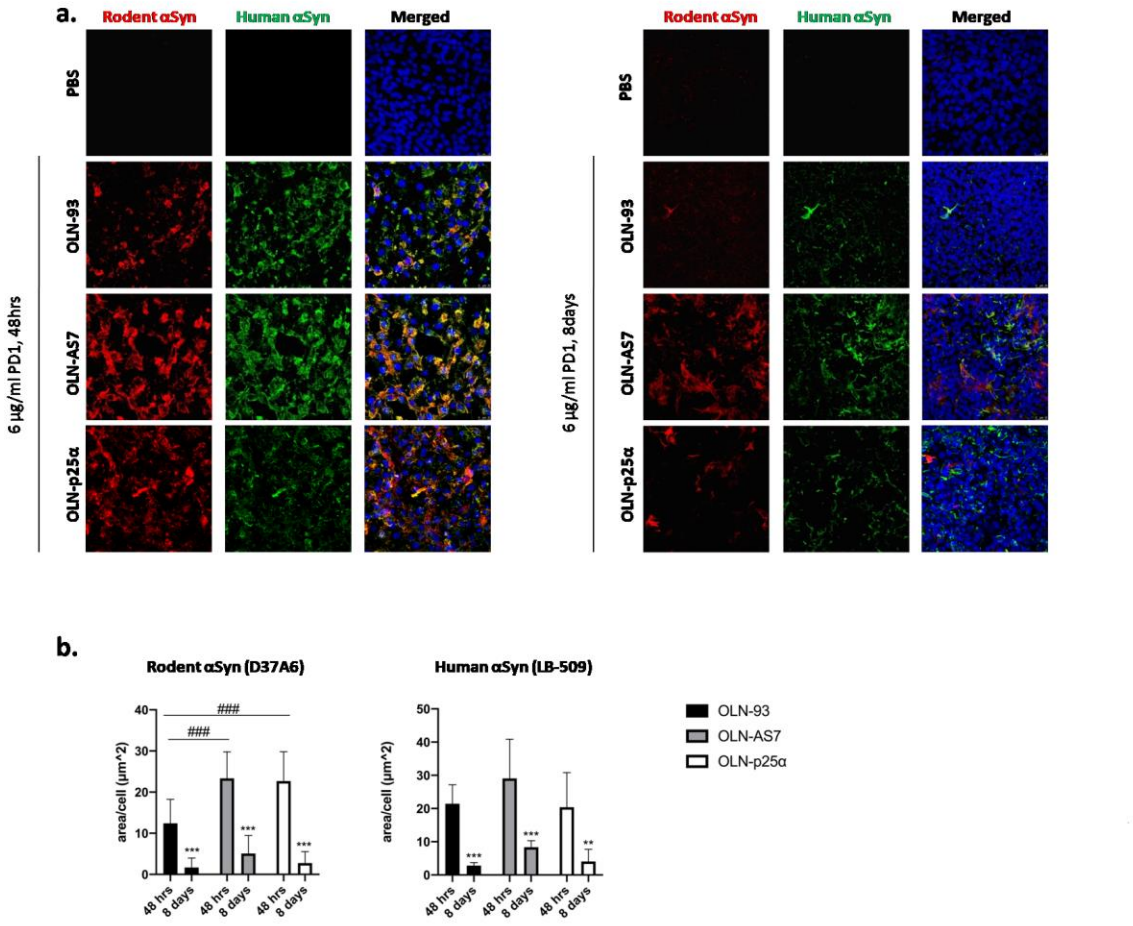

Figure 8 | High concentrations of PD1-patient derived fibrils seed the endogenous rodent αSyn. (8a) Representative immunofluorescence images using antibodies against human αSyn (**green**, LB-509) and endogenous rat αSyn (**red**, D37A6) in OLN-cell-lines treated with 6µg/ml of PD1 fibrils for 48 hours (left) or 8 days (right). DAPI staining is used as nuclear marker. Cells treated with PBS, in the absence of fibrils, were used as controls. Scale bar: 25µm.**(8b)** Quantifications of endogenous rat and human αSyn protein levels in OLN-cells expressed as area surface normalized to the total number of cells per image. Data are expressed as the mean ± SD of at least three independent experiments with triplicate samples/ condition within each experiment; *p<0.05; **p<0.01; ***p<0.001, comparing fibril-treated conditions within the same cell line and # p<0.05; ##p<0.01; #p<0.001, comparing between the different OLN-cell lines by two-way ANOVA with Bonferroni's-correction.

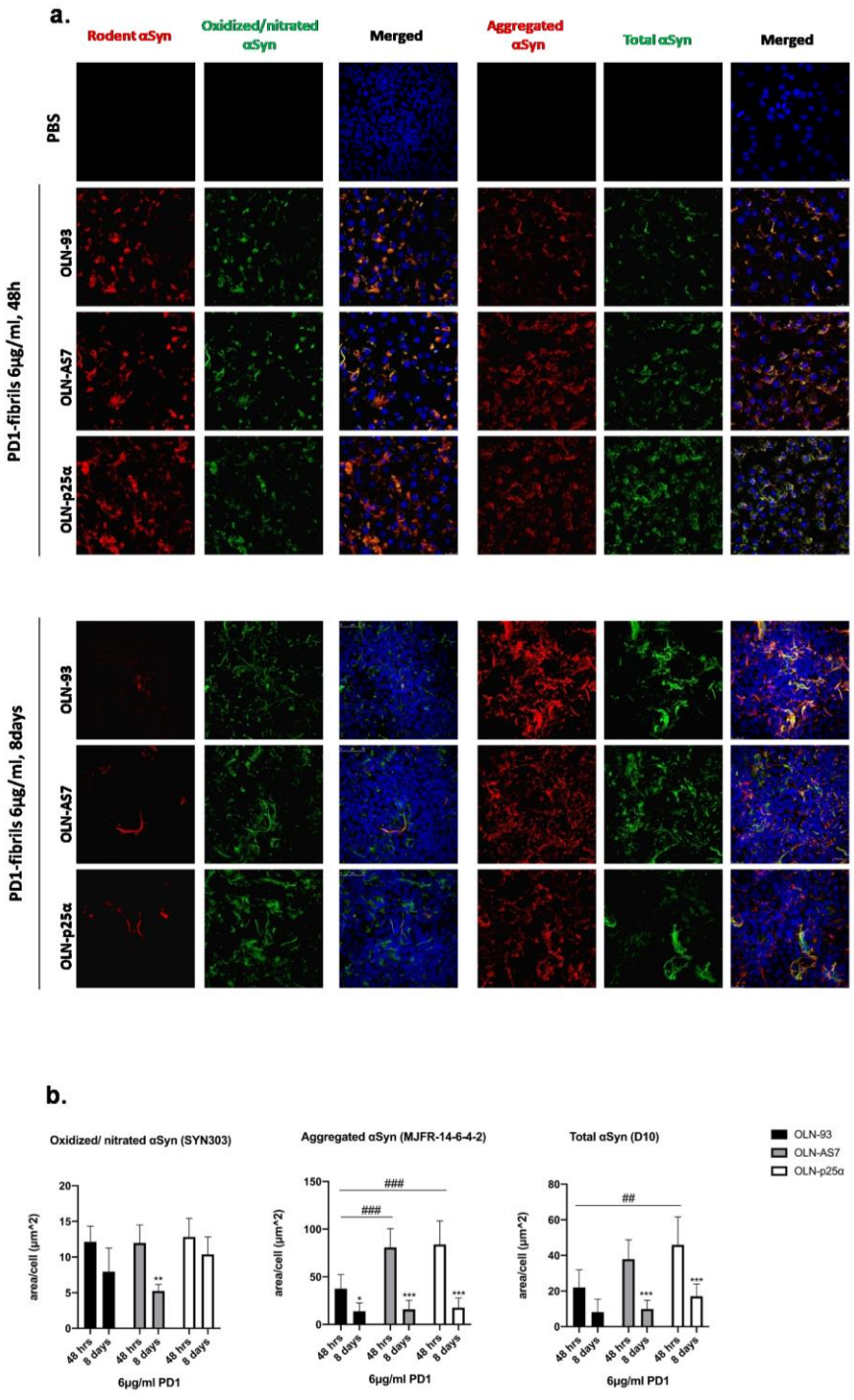

Figure 9 | High concentrations of PD1patient-derived fibrils evoke the formation of pathological αSyn species. (9a) Representative immunofluorescence images using antibodies against oxidized/nitrated αSyn (**green**, SYN303, first row), endogenous rodent αSyn (**red**, D37A6, second row), aggregated αSyn conformations (**red**, MJFR 14-6-4-2, forth row) and total αSyn (human and rodent, **green**, D10, fifth row) staining in OLN cells treated with 6 µg/ml of PD1 fibrils for 48 hours or 8 days. DAPI staining is used as nuclear marker. Scale bar: 25µm.**(9b)** Quantifications of oxidized/nitrated, aggregated and total αSyn protein levels in OLN-cells expressed as area surface normalized to the total number of cells per image. Data are expressed as the mean ± SD of at least three independent

experiments with triplicate samples/ condition within each experiment; *p<0.05; **p<0.01; ***p<0.001, comparing fibril-treated conditions within the same cell line and # p<0.05; ##p<0.01; #p<0.001, comparing between the different OLN-cell lines by two-way ANOVA with Bonferroni's-correction.

Addition of high concentrations of PD1 patient derived fibrils enhances the exosome-associated release of αSyn in OLN-AS7 cells

We next assessed the αSyn cargo and the quantity of exosomes secreted from OLN-AS7 cells treated with the higher fibril concentration as above. Oligodendroglial exosomes isolated from PD1 fibril-inoculated OLN-AS7 cells were found to carry both monomeric and HMW αSyn(Fig. 10a) and, rarely, truncated αSyn species. Quantification of the protein band detected in immunoblots revealed that the levels of human and total monomeric αSyn peaked at 48 hours and then decreased over time. Interestingly, HMW human αSyn species, remained at high levels in exosomes released from cells at 8 days post-fibril addition, possibly indicating that higher fibril concentration lead to the formation of relative more insoluble αSyn species intracellularly (Fig. 10b).Moreover, the amount of exosomes again measured by the acetylocholinesterase activity increased significantly at 48 hours post-fibril addition, probably suggesting that higher concentrations of PD fibrils facilitates the generation of highly aggregated protein species intracellularly, that the cell's protein quality control cannot remove and are then packed and secreted via exosomes (Fig. 10c).

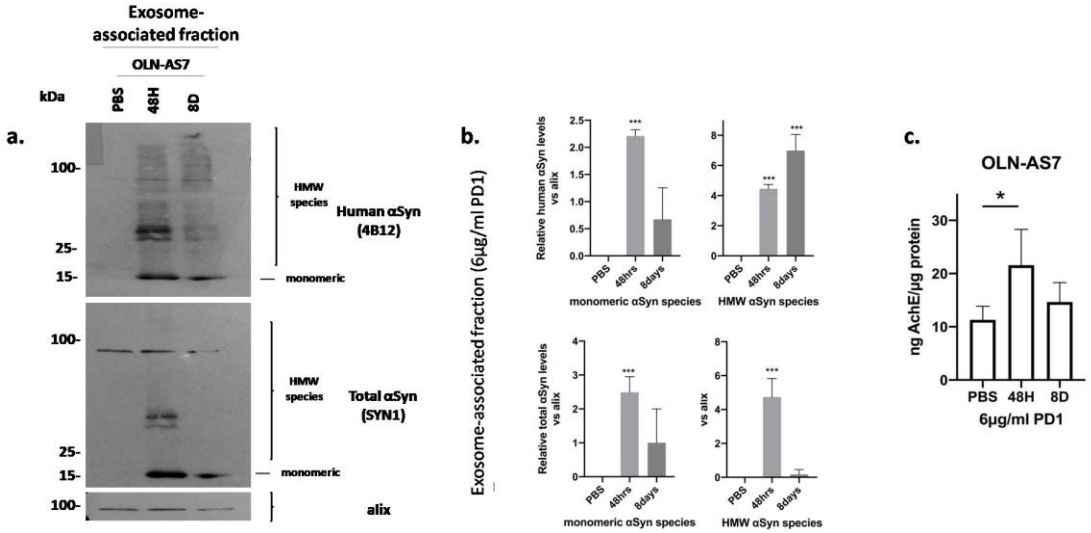

Figure 10 | Addition of high concentrations of PD1 patient-derived fibrils enhances the exosome-associated release of αSyn. (10a) Representative immunoblots of the exosome-associated fractions demonstrating the presence of both human (4B12 antibody) and total (SYN-1 antibody) αSyn (monomeric and high-molecular weight species) protein within exosomes.OLN-AS7 cells were treated with 6 µg/ml PD1-amplified fibrils for either 48hours or 8days.**(10b)** Quantifications of the exosome-associated levels of human (4B12 antibody) and total (SYN-1 antibody) αSyn. Equal loading is verified by the detection of the exosomal marker alix. Data are expressed as the mean ± SD of at least three independent experiments; *p<0.05; **p<0.01; ***p<0.001, comparing PBS- and fibril-treated conditions within the same cell line by unpaired t-test .**(10c)**Indirect quantification of the amounts of the exosomal vesicles derived from PBS- and PD1 fibril treated OLN-AS7 cells by measuring the activity of

acetylocholinesterase enzyme normalized to the total protein load. Data are expressed as the mean ± SD of at least three independent experiments.

High amounts of PD1 fibrils evoke the formation of Urea-soluble protein species of the endogenous rodent αSyn within OLN-AS7 cells and enhance its exosome-associated release

To further examine the propagation of αSyn pathology following PD fibril incubation of OLN-AS7 cells, we assessed the intracellular and exosome-associated levels of the seeded endogenous rodent αSyn, which is not detected under basal conditions. Using the lower amounts of PD1 fibrils, we were unable to detect any endogenous rodent αSyn in western immunoblotting, either intracellularly or extracellularly (data not shown). Contrariwise, higher PD1 fibril concentrations allowed the detection of the endogenous rodent αSyn, only in the Urea-soluble fraction, trapped in the stacking gel (Fig.11a).Likewise, endogenous rodent αSyn was also detected in the stacking gel of the exosome-associated fractions, thus suggesting that the oligodendroglial protein can be packed and secreted via exosomes (Fig.11b).Both intracellularly and in exosomes, rodent αSyn signal was detected at higher levels at 48 hours, compared to 8 days, post-fibril addition (Fig.11c,d).

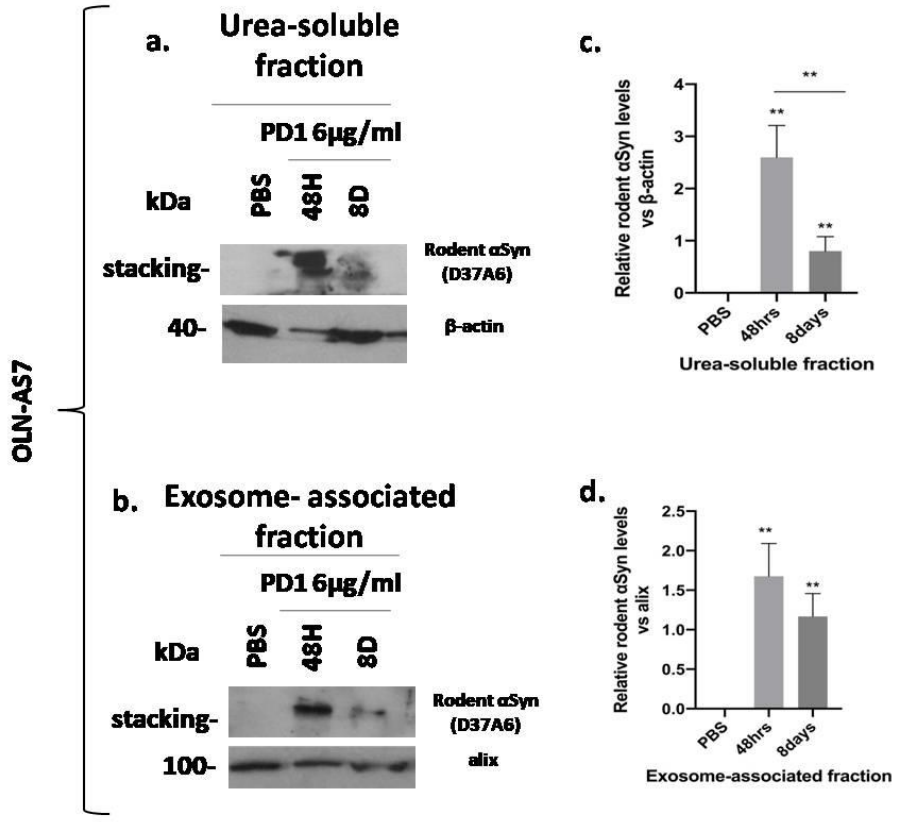

Figure 11 |The seeded endogenous oligodendroglialαSyn is detected in the Urea-soluble fraction intracellularly and is partly released via exosomes, following inoculation of OLN-AS7 cells with high amounts of PD1 fibrils. (12a) Representative immunoblots of the Urea-soluble fraction demonstrating the detection of the rodent

αSyn(D37A6) protein in OLN-AS7 cells treated with 6 μg/ml PD1-amplified fibrils for either 48hours or 8days.**(12b)** Representative immunoblots of the exosome-associated fraction demonstrating the presence of the endogenous rodent αSyn (D37A6) in OLN-AS7 cells treated with 6 μg/ml PD1-amplified fibrils for either 48hours or 8days.**(12c,d)** Quantifications of the Urea-soluble and exosome-associated levels of the endogenous rodent αSyn (D37A6). Equal loading is verified by the detection of the protein marker β-actin (for the Urea-soluble fraction) or the exosomal marker alix. Data are expressed as the mean ± SD of at least three independent experiments; *p<0.05; **p<0.01; ***p<0.001, comparing PBS- and fibril-treated conditions within the same cell line by unpaired t-test.

Addition of high amounts of PD fibrils in OLN-AS7 cells evokes the phosphorylation of αSyn at Ser129 and enhances its exosome associated release

Considering that the presence of phosphorylated at Ser129 αSyn represents a pathology-related post-translational modification widely used as a marker for alpha-synucleinopathies, we assessed pSer129 levels in OLN-AS7 cells treated with 6μg/ml PD1 fibrils for 48 hours and 8 days. Noteworthy, we were able to detect pSer129 αSyn protein only in the Urea-soluble fraction at both time points and strikingly, also in the exosome-associated fraction, detected at higher levels at 8 days post-fibril addition (Fig. 12a,b).Furthermore, immunofluorescence analysis, to all OLN-cell lines treated with high concentrations of PD1 fibrils for 48 hours and 8 days, verified the presence of pathology-related pSer129 αSyn only in cells with increased intracellular protein load (OLN-AS7 cells) both at 48 hours (data not shown) and 8 days (Fig. 12c).Finally, proof-of-concept analysis using sonicated fibrils was performed, as it has been previously mentioned that shorter fibril length results in higher seeding activity [88]. However, in our hands, sonication did not enhance the seeding capacity of the patient-derived fibrils as assessed by the recruitment of the endogenous protein and the formation of pathological assemblies (Fig. 13).In contrast, less immunofluorescence signal of endogenous seeded, aggregated and phosphorylated αSyn was detected in cells treated with the sonicated fibrils.

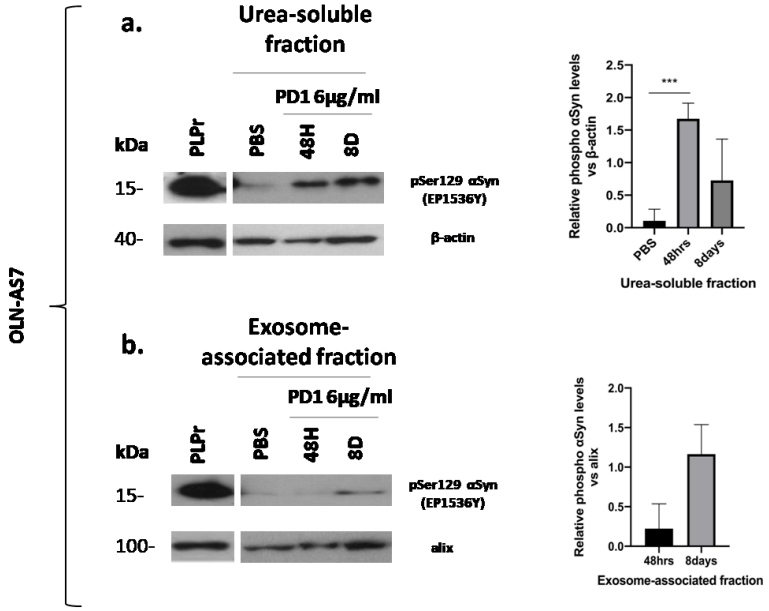

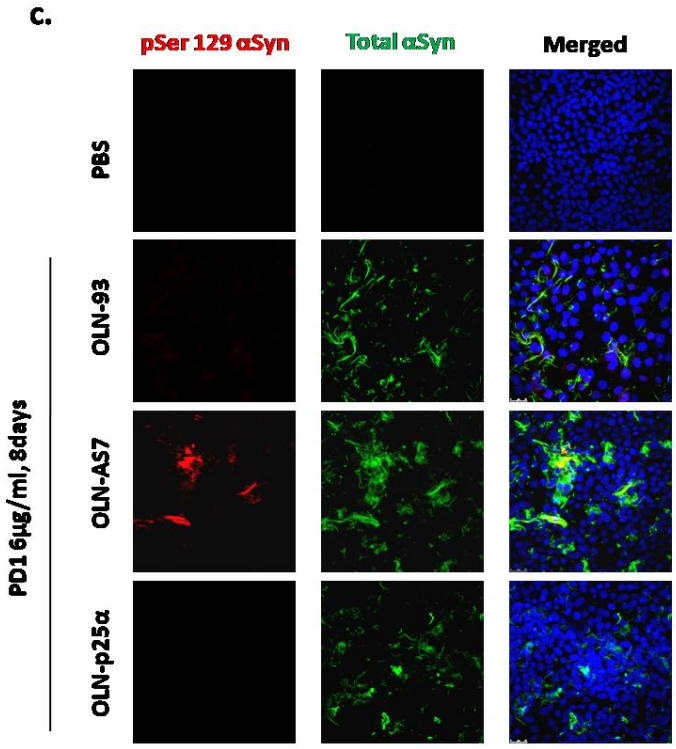

Figure 12 | Addition of high amounts of PD1 patient-derived evokes the pSer129 phosphorylation of αSyn and enhances its exosomes-associated release. (12a) Representative immunoblots (left) and quantification (right) of the Urea-soluble fraction demonstrating the presence of pSer129 αSyn (EP1536Y) in OLN-AS7 cells treated with 6 µg/ml PD1-amplified fibrils for either 48hours or 8days.**(12b)** Representative immunoblots (left) and quantification (right) of the exosome-associated fraction demonstrating the presence of pSer129 αSyn (EP1536Y) in exosomes released by OLN-AS7 cells treated with 6 µg/ml PD1-amplified fibrils for either 48hours or 8days. Equal loading is verified by the detection of the protein marker β-actin (for Urea-soluble fraction) or the exosomal marker alix (for exosome-associated fraction). In exosome-associated fraction results are normalized to the corresponding PBS signal. PLP brain lysate was used as a positive control. Data are expressed as the mean ± SE of at least three independent experiments; *p<0.05; **p<0.01; ***p<0.001, comparing PBS- and fibril-treated conditions within the same cell line by unpaired t-test. **(12c)** Representative immunofluorescence images using antibodies against pSer129 (**red**, EP1536Y) and total αSyn (human and rodent, **green**, D10) proteins in OLN-AS7 cells treated with 6µg/ml of PD1 fibrils for 8 days. DAPI staining is used as nuclear marker. Scale bar: 25µm.

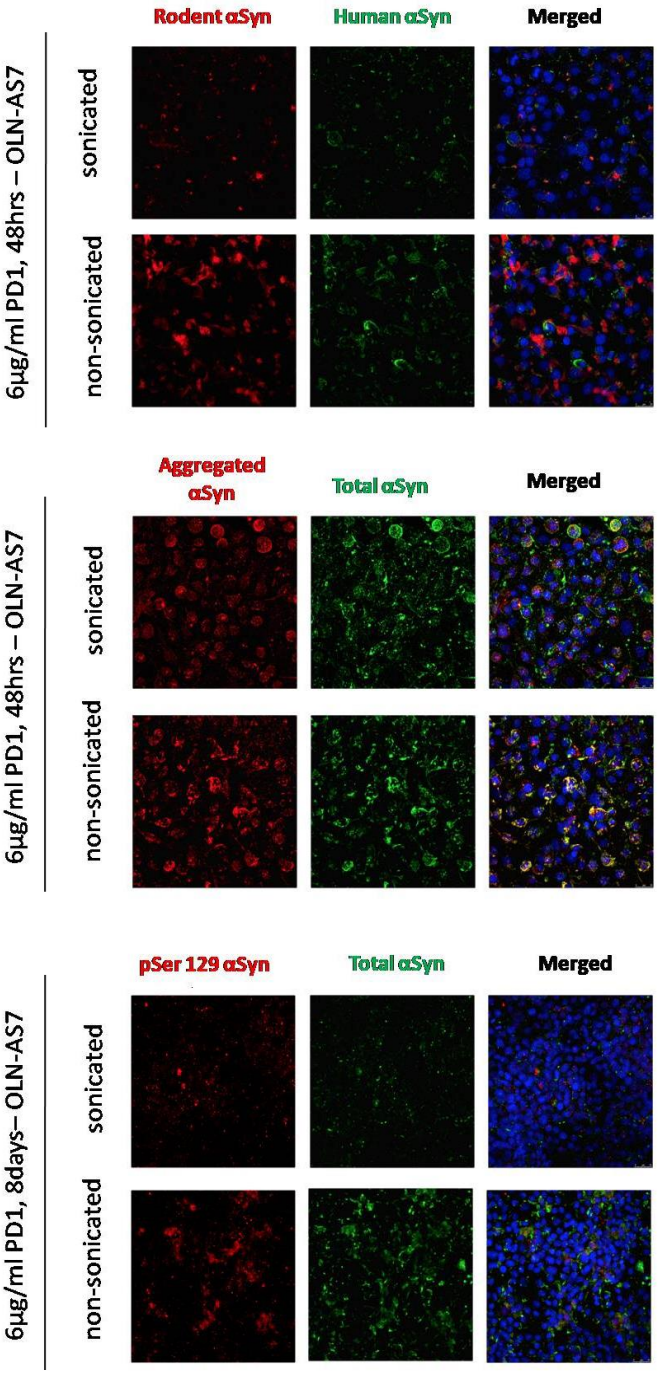

Figure 13 | Sonication of PD1 fibrils does not improve the seeding capacity of PD patient-derived fibrils. Representative immunofluorescence images using antibodies against the endogenous rodent (**red**, D37A6), human (**green**, LB-509), aggregated (**red**, MJFR 14-6-4-2), pSer129 (**red**, EP1536Y) and total αSyn (human and rodent, **green**, D10) αSyn conformations in OLN-AS7 cells treated with 6µg/ml of PD1 fibrils for 48 hours or 8 days. DAPI staining is used as nuclear marker. Scale bar: 25µm.

Effects of human PD1 patient-amplified fibrils on p25α levels and distribution over time

Finally, given the strong correlation of αSyn and TPPP/p25α interplay in the establishment of MSA-like pathology, we examined p25α levels intracellularly and extracellularly, upon addition of1 μg/ml PD1 fibrils in OLN-p25α cells for 48 hours and 8 days. Interestingly, intracellular (Triton-, SDS-, Urea- soluble fractions) p25α levels displayed a statistically significant drop at 48 hours post-fibril addition, followed by a partial recovery at 8 days (Fig. 14a,b). Contrariwise, exosomal p25α levels increased upon fibril addition, following both short and prolonged incubation, as compared to baseline conditions (Fig. 14a,b). This result probably indicates that the αSyn species produced in fibril-treated OLN-p25α cells promote the degradation of the protein as a response to proteolytic stress and/or accelerate p25α secretion, at least partly, via exosomes. To further examine whether indeed intracellular degradation systems are responsible for the p25α drop at 48 hours, we used NH_4Cl, a general inhibitor of lysosomal proteolysis (Fig. 14c). Strikingly, upon lysosomal inhibition p25α levels were restored intracellularly, reaching baseline levels, suggesting that the lysosome is partly responsible for the protein degradation under these conditions. Finally, we assessed the impact of PD fibrils addition on p25α levels and distribution by immunofluorescence analysis. Noteworthy, we noticed that p25α network collapses upon addition of PD1 fibrils, as the well-shaped p25α protein motif in PBS-treated cells, becomes not only diffused but also punctuated in PD1 fibril-treated cultures (Fig. 14d). Interestingly, aberrant p25α fibrillar-like conformations co-localized with the endogenous rodent and human αSyn, thus pinpointing its incorporation in pathological αSyn assemblies.

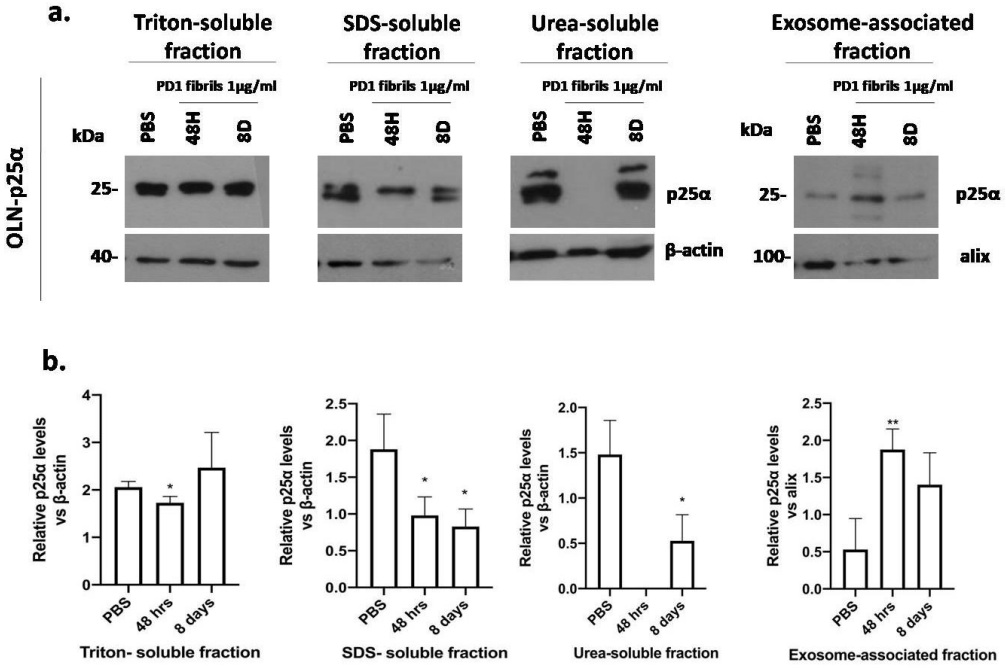

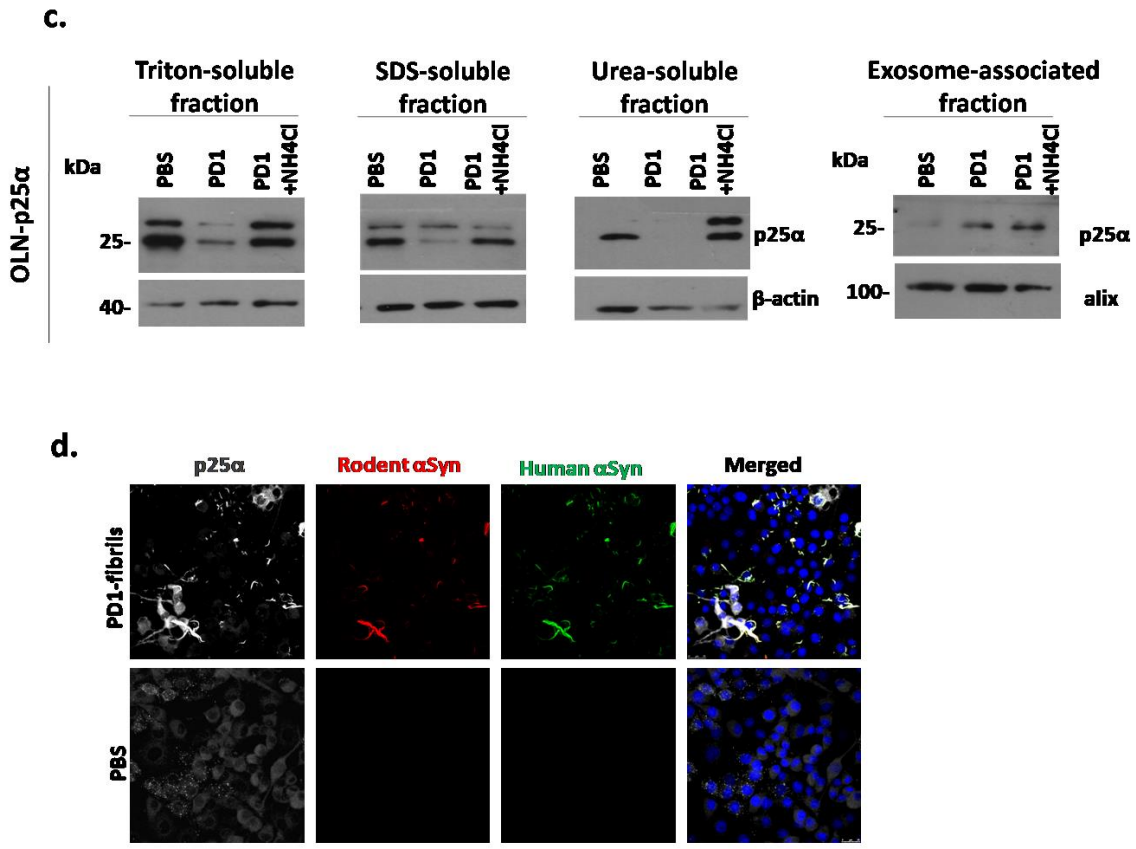

Figure 14 | Effects of human PD1 patient-amplified fibrils on p25α levels and distribution over time. (14a) Representative immunoblots demonstrating the effects of αSyn PD1-patient amplified fibrils on intracellular (Triton-, SDS- and UREA- soluble fractions) and exosome-associated p25α protein levels.**(14b)** Quantifications of p25α levels intracellularly (Triton-, SDS-, Urea- soluble fractions) and in exosome-associated fraction. Data are expressed as the mean ± SD of at least three independent experiments; *p<0.05; **p<0.01; ***p<0.001, comparing PBS- and fibril-treated conditions within the same cell line by unpaired t-test. Equal loading is verified by the detection of the protein marker β-actin. **(14c)** Representative immunoblots demonstrating the effects of NH_4Cl, a known inhibitor of lysosomal proteolysis, to p25α levels in PD1-patient derived treated OLN-p25α cells (1 µg/ml, 48h).**(14d)** Representative immunofluorescence images depicting the redistribution of p25α (**grey**) and the presence of human αSyn (**green**, LB-509) and endogenous rat αSyn (**red**, D37A6) signal in OLN-p25α cells treated with 1µg/ml of PD1 fibrils for 48 hours. DAPI staining is used as nuclear marker. Cells treated with PBS, in the absence of fibrils, were used as controls. Scale bar: 25µm.

Discussion

MSA is a debilitating, unique alpha-synucleinopathy, characterized by the presence of αSyn-positive proteinaceous inclusions (GCIs) within oligodendrocytes[7]. Interestingly, growing body of evidence favors the idea of the existence of distinct αSyn strains present in neuronal (PD, DLB) and oligodendroglial (MSA) synucleinopathies that underlie disease development and heterogeneity. In particular, αSyn is often considered as a prion-like agent, able to self-propagate through seeding of the endogenous protein and to acquire pathological conformations capable of cell-to-cell transmission of pathology [89]. Indeed, MSA brain extracts containing pathological αSyn when intrastriatally inoculated into mice expressing human wild-type αSyn lead to the formation of pathology-related αSyn species, supporting the prion-like transmission of αSyn-related pathology in MSA [90]. Interestingly, emerging evidence also favors the "strain hypothesis", where distinct structural αSyn conformations could underlie the presence of diseases with unique clinical and histopathological phenotypes, within alpha-synucleinopathies[91-94]. In support of this scenario, recent studies also demonstrate that αSyn strains exhibit distinct structural and biological characteristics and that oligodendroglial but not neuronal milieu, transforms misfolded neuronally-derived αSyn into GCI-like species, which are more prone to seed the pathology in primary neurons [95]. Additionally, several reports have pinpointed selective conformational and biochemical differences within aggregates of αSyn derived from patients diagnosed with distinct synucleinopathies[84, 93, 96-99].

The origin of αSyn in oligodendroglial cells raised fundamental questions, as initial studies showed that mature oligodendrocytes do not normally express the protein. However, subsequent studies have reported that the protein may be expressed in oligodendrocytes, albeit at significantly lower levels compared to those observed in neurons, which are the cells that physiologically express the protein [31, 32, 40, 41]. Nevertheless, the prevailing hypothesis explaining the presence of neuronal αSyn in mature oligodendrocytes, suggests that the protein is released from neurons and is subsequently taken up by oligodendrocytes, present in their surroundings, even though the precise mechanisms still remain rather ambiguous[33, 35, 36, 38]. Different preclinical studies have demostrated the ability of oligodendrocytes to take-up exogenously added recombinant or neuronally-derived, cell produced, αSyn and to incorporate it into intracellular GCI-like aggregates [35-38]. Once successful internalization of αSyn by recipient cells has occurred, the exogenously-added material has been shown to seed the accumulation of the endogenous protein [100, 101].

Herein, we report that human αSyn fibrils amplified from the brains of two PD patients can be taken up by rodent oligodendroglial cells *in vitro*. Interestingly, structural differences between the two different fibril types were observed (Fig.1), possibly reflecting the great variability of disease phenotypes present in PD patients. This is in agreement with previous analyses on patient-derived fibrils that question the correlation of a particular αSyn strain with a particular synucleinopathy [84]. Nonetheless, such discrepancies could also be attributed to technical differences during the fibril preparation procedure. However, to what extent these structural differences are also accompanied by distinct biological effects remains to be proven. Our data also show that PD patient-derived fibrils, probably of neuronal origin, induce the formation of pathological αSyn assemblies within oligodendrocytes that incorporate the endogenous rodent αSyn, expressed at minute amounts under basal conditions, as previously reported to occur when human recombinant PFFs were used as seeds [25]. Interestingly, using lower amounts of patient-derived fibrils we were able to detect the endogenous rodent αSyn signal only via immunofluorescence, and not by western immunoblotting, highlighting perhaps the differences in methods' sensitivity. Contrariwise, using higher fibril amounts, we detected the endogenous rodent αSyn present only in the Urea-soluble fraction, probably reflecting its highly aggregated form. Regarding

the human αSyn, Triton-soluble and –insoluble αSyn species were found to peak following short-term incubation with PD fibrils. Interestingly, in OLN-AS7 and OLN-p25α cells human and total αSyn levels remained relatively higher as compared to OLN-93 control cells at 48 hours and 8 days, thus highlighting the important role of αSyn and/or p25α intracellular protein load on the establishment of MSA-like pathology and possibly indicating a relative resistance to degradation of αSyn species generated in the cells that overexpress human αSyn or p25α, respectively (Fig.2b,c, Fig.7a,b). Statistical analysis within each cell line, pinpointed a significant reduction of αSyn levels at 8 days, as compared to the earlier time-point (Fig.3, 8). This could be attributed to the dilution of the exogenously added human material following cell proliferation or its effective clearance by the intracellular proteolytic mechanisms.

Release and uptake of αSyn between cells can occur through different mechanisms; however the role of extracellular vesicles, especially exosomes, has recently gained significant interest [50, 51, 102]. Multiple studies have shown that both neurons and glial cells are able to release and internalize exosome-related αSyn[50, 51, 103]. Interestingly, this exosome-associated αSyn is reported to be more prone to aggregation than cytosolic αSyn, and exosomes derived from the CSF of PD patients show higher seeding potency compared to healthy controls [50, 104]. Except from CSF, αSyn has been also found in other biological fluids including saliva, plasma and red blood cells [44, 102, 105-107] and tremendous focus has been given into using extracellular αSyn as a biomarker for alpha-synucleinopathies, although more research needs to be done, as results often appear contradictory [108-110]. Herein, we demonstrate that αSyn species engendered within PD-fibril treated oligodendroglial cells, are released in the extracellular environment via exosomes (Fig.5). In these isolated exosomes, we identified both monomeric as well as HMW αSyn conformations (Fig.6). Interestingly, exosome-associated HMW human αSyn levels derived from OLN-AS7 cells treated with high PD-derived fibril amounts, remained high, even after 8 days post-fibril treatment, possibly reflecting the presence of relatively more aggregated, rather insoluble, αSyn species intracellularly (Fig.10). Interestingly, not only the exogenously added human protein but also the endogenous seeded rodent αSyn was also detected in exosomes released from OLN cells treated with PD fibrils, suggesting that the oligodendroglial protein can be packed and secreted via exosomes (Fig.11)

To further examine whether the endogenous rodent αSyn is incorporated into pathological αSyn assemblies following the addition of PD patient-derived fibrils, we assessed the formation of pathological αSyn species. The phosphorylation of αSyn both at Ser129 is widely considered as an indicator of pathology, but contradictory studies on its actual effects is still under debate [111-118]. In Lewy Bodies, the histopathological hallmark for PD, 90% of αSyn is found to be phosphorylated at Ser129, but a significant amount of phosphorylated Ser129 αSyn is also detected in a soluble, rather than in an aggregated state in PD brains [119], whereas only low levels of aSyn phosphorylation at Ser129 is detected in the brains of healthy controls [120-122]. Still, in the majority of *in vivo* models where αSynis overexpressed, the presence of pSer129 αSyn is mostly connected to neurotoxic, rather than neuroprotective, effects. Ongoing comparative analysis in the host lab of the presence of Ser129 αSyn phosphorylation in oligodendroglial cells treated with either MSA or PD patient-derived fibrils, further favors the notion that synucleinopathies are caused by different αSyn strains. Indeed, PD-fibrils lead to the pSer129 αSyn only in OLN-AS7 cells(Fig.12), whereas, with MSA-fibrils we mostly observe phosphorylation in OLN-p25α cells (data not shown). Such data may indicate that fibrils amplified from PD patients which have a neuronal origin, tend to preferentially affect cells that overexpress αSyn (OLN-AS7), whereas fibrils derived from MSA patients, that have an oligodendroglial origin, mostly aggregate and become pathological in cells that overexpress p25α (OLN-p25α), the protein that together with αSyn accumulate in GCIs. Moreover, using PD fibrils we were able to detect intracellular positive pSer129 αSyn signal only in the Urea-soluble fraction of OLN-AS7 cells, whereas exosome-associated pSer129

αSyn was also detected, mainly at 8 days, showing that this pathological protein conformations can indeed be packed and secreted via extracellular vesicles, and probably transmit the pathology in neighboring cells (Fig.12).

Beyond phosphorylation, αSyn nitration has been also associated to neurodegeneration, as proven by experiments both *in vitro* and *in vivo*, as well as by human neuropathological studies[123-125], possibly through its role in oxidative damage and disease progression [126]. In our experimental model, we observed the formation of oxidized/nitrated αSyn in all OLN-cells treated with 1 or 6μg/ml PD-derived fibrils that co-localized with the rodent protein, thus highlighting the contribution of the endogenous oligodendroglial αSyn in the generation of pathology-related species intracellularly (Fig.4, 9). Interestingly, following incubation with 6μg/ml PD fibrils, SYN303-positive signal recognizing the oxidized/nitrated protein was particularly persistent at 8 days, even though the levels of the rodent-specific protein decreased in all OLN-cell lines. This observation may indicate that the exogenously added human patient-derived material becomes modified intracellularly. However, this cannot be tested with a double immunostaining using the human-specific and oxidized/nitrated αSyn antibodies due to the fact that both of them are mouse monoclonal. However, a time-course analysis incorporating earlier time-points (1, 2, 8, 12 hrs post-fibril addition) may enable the mapping of αSyn pathology established by the addition of PD fibrils in OLN cells, as previously performed in cells treated with PFFs [25].

Finally, αSyn truncation, especially in the carboxyl-terminal region, has been shown to have a critical role in the pathological misfolding and subsequent seeding activity of the protein (review in [127]). Indeed, 20% of αSyn is being C-terminally truncated within pathologic inclusion extracts[128-131]. The effects of truncated αSyn in pathophysiological processes have been assessed in both preclinical models and in patient-derived post-mortem samples. It is indeed evident that truncated αSyn is involved in the formation of toxic αSyn aggregates[129, 132, 133]. The C-terminus of αSyn is associated with multiple protective characteristics to limit aberrant misfolding and aggregation, and its loss through truncation promotes *in vitro* oligomer and fibril formation, strikingly in higher levels than the full-length αSyn[50, 129, 133-142]. Moreover, it has been demonstrated that αSyn fibrils added in neuronal cells are quickly transferred for lysosomal processing, where extensive truncation can easily occur[143-145]. Also, different studies have shown that endogenous αSyn is mainly degraded through autophagy-related pathways[146, 147], contrariwise to pathologic αSyn fibrils that are trafficked to lysosomes for elimination by cathepsins[143-145, 148]. In both cases, proteases act on αSyn and can subsequently lead to disease-related truncations. These proteases may be directly linked to pathology, as some of them have been found to colocalize with LBs or GCIs[139, 149-151].Noteworthy, the vast majority of studies focusing on truncation are implemented on PD and not MSA [119, 152]. In our study, we detected truncated αSyn species both intracellularly and extracellularly, associated with exosomes, but not consistently. Additional experiments are needed to further elucidate the presence of truncated αSyn in our experimental set-up, as well as its potential role, if any, on the onset and progression of MSA-like pathology.

Beyond αSyn, the oligodendroglial specific phosphoprotein TPPP/p25α is also found trapped in GCIs and it is hypothesized that the protein mislocalizes from the oligodendroglial processes to the abnormally expanded cell soma, prior to αSyn accumulation [8, 19, 20, 23]. Indeed, *in vitro* experiments showed that this protein regulates the aggregation of αSyn and interferes with its lysosomal degradation, leading to enhanced levels of αSyn in the cell medium. However, direct evidence for the involvement of TPPP/p25α in MSA onset and development still remains insufficient [23, 24]. Recently published work from the host lab revealed a crucial role for TPPP/p25α in the recruitment and seeding of oligodendroglial αSyn and in the formation of aberrant aSyn species within oligodendrocytes treated

with human recombinant fibrils [25]. Herein, we demonstrate that PD-patient amplified aSyn fibrils evoke a drop on intracellular p25α levels at 48 hours, which is restored upon lysosomal inhibition. However, at the same time point exosomal p25α levels seem to increase, probably indicating that PD fibrils promote the lysosomal degradation of the protein and its secretion partly via exosomes. Such data may also indicate that p25α propagates from one cell to the other, thus facilitating the aggregation of αSyn in recipient cells. In a recently published paper from the host lab where pharmacological and molecular inhibition of both autophagic and proteasomal pathways was employed, it has been reported that the endogenous oligodendroglial p25α is mostly degraded by the autophagy-lysosome pathway in OLN cell lines and primary oligodendrocytes[153]. Previous studies have proposed that p25α is also degraded via the proteasome [21, 154]. Further experiments utilizing proteasomal modulators may shed light to the contribution of the proteasome on p25α protein degradation and release, following treatment of oligodendroglial cells with PD patient-derived fibrils.

Collectively, our study reveals that inoculation of oligodendroglial cell lines with PD patient-derived αSyn fibrils, recapitulated critical aspects of MSA pathogenesis. In particular, we showed the formation of rather insoluble, pathological αSyn species intracellularly, incorporating the endogenous oligodendroglial αSyn and the release of such pathology-related protein conformations partly via exosomes. More importantly, this line of research highlights a critical correlation of oligodendroglial-derived exosomes and αSyn and p25α cargoes upon PD fibril treatment, that up-to-now have been narrowly explored. More experiments are needed to further elucidate the specific role of such oligodendroglia-derived exosomes in the transmission of MSA pathology. Since currently, synucleinopathy-related research on exosomes is targeted mostly in PD, it is highly important to understand the contribution of exosomes on the initiation and progression of MSA-like pathology. Corroboration of our hypothesis will provide valuable knowledge to better understand and attenuate MSA disease progression. Moreover, targeting oligodendroglial-derived exosomes may open up new ways to alter disease progression, since up-to-date there are no efficient disease-modifying therapies, nor accurate disease-specific biomarkers.

References

1. Fanciulli, A. and G.K. Wenning, *Multiple-system atrophy.* N Engl J Med, 2015. **372**(3): p. 249-63.
2. Wenning, G.K., et al., *Multiple system atrophy: sporadic or familial?* Lancet, 1993. **342**(8872): p. 681.
3. Spillantini, M.G. and M. Goedert, *Synucleinopathies: past, present and future.* Neuropathol Appl Neurobiol, 2016. **42**(1): p. 3-5.
4. Papp, M.I., J.E. Kahn, and P.L. Lantos, *Glial cytoplasmic inclusions in the CNS of patients with multiple system atrophy (striatonigral degeneration, olivopontocerebellar atrophy and Shy-Drager syndrome).* J Neurol Sci, 1989. **94**(1-3): p. 79-100.
5. Spillantini, M.G., et al., *alpha-Synuclein in filamentous inclusions of Lewy bodies from Parkinson's disease and dementia with lewy bodies.* Proc Natl Acad Sci U S A, 1998. **95**(11): p. 6469-73.
6. Jellinger, K.A. and P.L. Lantos, *Papp-Lantos inclusions and the pathogenesis of multiple system atrophy: an update.* Acta Neuropathol, 2010. **119**(6): p. 657-67.
7. Trojanowski, J.Q., T. Revesz, and M.S.A. Neuropathology Working Group on, *Proposed neuropathological criteria for the post mortem diagnosis of multiple system atrophy.* Neuropathol Appl Neurobiol, 2007. **33**(6): p. 615-20.

8. Wenning, G.K., et al., *Multiple system atrophy: a primary oligodendrogliopathy.* Ann Neurol, 2008. **64**(3): p. 239-46.
9. Spillantini, M.G., et al., *Alpha-synuclein in Lewy bodies.* Nature, 1997. **388**(6645): p. 839-40.
10. Wakabayashi, K., et al., *Accumulation of alpha-synuclein/NACP is a cytopathological feature common to Lewy body disease and multiple system atrophy.* Acta Neuropathol, 1998. **96**(5): p. 445-52.
11. Wakabayashi, K., et al., *Alpha-synuclein immunoreactivity in glial cytoplasmic inclusions in multiple system atrophy.* Neurosci Lett, 1998. **249**(2-3): p. 180-2.
12. Nakamura, K., et al., *Filamentous aggregations of phosphorylated alpha-synuclein in Schwann cells (Schwann cell cytoplasmic inclusions) in multiple system atrophy.* Acta Neuropathol Commun, 2015. **3**: p. 29.
13. Gai, W.P., et al., *alpha-Synuclein fibrils constitute the central core of oligodendroglial inclusion filaments in multiple system atrophy.* Exp Neurol, 2003. **181**(1): p. 68-78.
14. Jellinger, K.A., *Young-onset multiple system atrophy.* Mov Disord, 2018. **33**(12): p. 1974-1975.
15. Papp, M.I. and P.L. Lantos, *The distribution of oligodendroglial inclusions in multiple system atrophy and its relevance to clinical symptomatology.* Brain, 1994. **117 (Pt 2)**: p. 235-43.
16. Yoshida, M., *Multiple system atrophy: alpha-synuclein and neuronal degeneration.* Neuropathology, 2007. **27**(5): p. 484-93.
17. Jellinger, K.A., *P25alpha immunoreactivity in multiple system atrophy and Parkinson disease.* Acta Neuropathol, 2006. **112**(1): p. 112.
18. Ozawa, T., et al., *The spectrum of pathological involvement of the striatonigral and olivopontocerebellar systems in multiple system atrophy: clinicopathological correlations.* Brain, 2004. **127**(Pt 12): p. 2657-71.
19. Ettle, B., et al., *alpha-Synuclein-induced myelination deficit defines a novel interventional target for multiple system atrophy.* Acta Neuropathol, 2016. **132**(1): p. 59-75.
20. Song, Y.J., et al., *p25alpha relocalizes in oligodendroglia from myelin to cytoplasmic inclusions in multiple system atrophy.* Am J Pathol, 2007. **171**(4): p. 1291-303.
21. Lehotzky, A., et al., *Dynamic targeting of microtubules by TPPP/p25 affects cell survival.* J Cell Sci, 2004. **117**(Pt 25): p. 6249-59.
22. Kovacs, G.G., et al., *Natively unfolded tubulin polymerization promoting protein TPPP/p25 is a common marker of alpha-synucleinopathies.* Neurobiol Dis, 2004. **17**(2): p. 155-62.
23. Lindersson, E., et al., *p25alpha Stimulates alpha-synuclein aggregation and is co-localized with aggregated alpha-synuclein in alpha-synucleinopathies.* J Biol Chem, 2005. **280**(7): p. 5703-15.
24. Ejlerskov, P., et al., *Tubulin polymerization-promoting protein (TPPP/p25alpha) promotes unconventional secretion of alpha-synuclein through exophagy by impairing autophagosome-lysosome fusion.* J Biol Chem, 2013. **288**(24): p. 17313-35.
25. Mavroeidi, P., et al., *Endogenous oligodendroglial alpha-synuclein and TPPP/p25alpha orchestrate alpha-synuclein pathology in experimental multiple system atrophy models.* Acta Neuropathol, 2019. **138**(3): p. 415-441.
26. Iwai, A., et al., *The precursor protein of non-A beta component of Alzheimer's disease amyloid is a presynaptic protein of the central nervous system.* Neuron, 1995. **14**(2): p. 467-75.
27. Lashuel, H.A., et al., *The many faces of alpha-synuclein: from structure and toxicity to therapeutic target.* Nat Rev Neurosci, 2013. **14**(1): p. 38-48.
28. Maroteaux, L., J.T. Campanelli, and R.H. Scheller, *Synuclein: a neuron-specific protein localized to the nucleus and presynaptic nerve terminal.* J Neurosci, 1988. **8**(8): p. 2804-15.
29. Burre, J., et al., *Alpha-synuclein promotes SNARE-complex assembly in vivo and in vitro.* Science, 2010. **329**(5999): p. 1663-7.

30. Chen, R.H.C., et al., *Correction: alpha-Synuclein membrane association is regulated by the Rab3a recycling machinery and presynaptic activity.* J Biol Chem, 2020. **295**(41): p. 14248.
31. Djelloul, M., et al., *Alpha-Synuclein Expression in the Oligodendrocyte Lineage: an In Vitro and In Vivo Study Using Rodent and Human Models.* Stem Cell Reports, 2015. **5**(2): p. 174-84.
32. Asi, Y.T., et al., *Alpha-synuclein mRNA expression in oligodendrocytes in MSA.* Glia, 2014. **62**(6): p. 964-70.
33. Ettle, B., et al., *Intracellular alpha-synuclein affects early maturation of primary oligodendrocyte progenitor cells.* Mol Cell Neurosci, 2014. **62**: p. 68-78.
34. Kaji, S., et al., *Pathological Endogenous alpha-Synuclein Accumulation in Oligodendrocyte Precursor Cells Potentially Induces Inclusions in Multiple System Atrophy.* Stem Cell Reports, 2018. **10**(2): p. 356-365.
35. Kisos, H., et al., *Increased neuronal alpha-synuclein pathology associates with its accumulation in oligodendrocytes in mice modeling alpha-synucleinopathies.* PLoS One, 2012. **7**(10): p. e46817.
36. Konno, M., et al., *Suppression of dynamin GTPase decreases alpha-synuclein uptake by neuronal and oligodendroglial cells: a potent therapeutic target for synucleinopathy.* Mol Neurodegener, 2012. **7**: p. 38.
37. Reyes, J.F., et al., *Alpha-synuclein transfers from neurons to oligodendrocytes.* Glia, 2014. **62**(3): p. 387-98.
38. Rockenstein, E., et al., *Neuronal to oligodendroglial alpha-synuclein redistribution in a double transgenic model of multiple system atrophy.* Neuroreport, 2012. **23**(4): p. 259-64.
39. Richter-Landsberg, C., et al., *alpha-synuclein is developmentally expressed in cultured rat brain oligodendrocytes.* J Neurosci Res, 2000. **62**(1): p. 9-14.
40. Solano, S.M., et al., *Expression of alpha-synuclein, parkin, and ubiquitin carboxy-terminal hydrolase L1 mRNA in human brain: genes associated with familial Parkinson's disease.* Ann Neurol, 2000. **47**(2): p. 201-10.
41. Miller, D.W., et al., *Absence of alpha-synuclein mRNA expression in normal and multiple system atrophy oligodendroglia.* J Neural Transm (Vienna), 2005. **112**(12): p. 1613-24.
42. Jin, H., et al., *Analyses of copy number and mRNA expression level of the alpha-synuclein gene in multiple system atrophy.* J Med Dent Sci, 2008. **55**(1): p. 145-53.
43. Borghi, R., et al., *Full length alpha-synuclein is present in cerebrospinal fluid from Parkinson's disease and normal subjects.* Neurosci Lett, 2000. **287**(1): p. 65-7.
44. El-Agnaf, O.M., et al., *Detection of oligomeric forms of alpha-synuclein protein in human plasma as a potential biomarker for Parkinson's disease.* FASEB J, 2006. **20**(3): p. 419-25.
45. Braak, H., et al., *Staging of brain pathology related to sporadic Parkinson's disease.* Neurobiol Aging, 2003. **24**(2): p. 197-211.
46. Dickson, D.W., et al., *Evidence in favor of Braak staging of Parkinson's disease.* Mov Disord, 2010. **25 Suppl 1**: p. S78-82.
47. Woerman, A.L., et al., *alpha-Synuclein: Multiple System Atrophy Prions.* Cold Spring Harb Perspect Med, 2018. **8**(7).
48. Pukass, K. and C. Richter-Landsberg, *Oxidative stress promotes uptake, accumulation, and oligomerization of extracellular alpha-synuclein in oligodendrocytes.* J Mol Neurosci, 2014. **52**(3): p. 339-52.
49. Pukass, K., O. Goldbaum, and C. Richter-Landsberg, *Mitochondrial impairment and oxidative stress compromise autophagosomal degradation of alpha-synuclein in oligodendroglial cells.* J Neurochem, 2015. **135**(1): p. 194-205.
50. Lee, H.J., S. Patel, and S.J. Lee, *Intravesicular localization and exocytosis of alpha-synuclein and its aggregates.* J Neurosci, 2005. **25**(25): p. 6016-24.

51. Emmanouilidou, E., et al., *Cell-produced alpha-synuclein is secreted in a calcium-dependent manner by exosomes and impacts neuronal survival.* J Neurosci, 2010. **30**(20): p. 6838-51.
52. Danzer, K.M., et al., *Exosomal cell-to-cell transmission of alpha synuclein oligomers.* Mol Neurodegener, 2012. **7**: p. 42.
53. Fevrier, B., et al., *Cells release prions in association with exosomes.* Proc Natl Acad Sci U S A, 2004. **101**(26): p. 9683-8.
54. Mathivanan, S., H. Ji, and R.J. Simpson, *Exosomes: extracellular organelles important in intercellular communication.* J Proteomics, 2010. **73**(10): p. 1907-20.
55. Doyle, L.M. and M.Z. Wang, *Overview of Extracellular Vesicles, Their Origin, Composition, Purpose, and Methods for Exosome Isolation and Analysis.* Cells, 2019. **8**(7).
56. Ratajczak, J., et al., *Embryonic stem cell-derived microvesicles reprogram hematopoietic progenitors: evidence for horizontal transfer of mRNA and protein delivery.* Leukemia, 2006. **20**(5): p. 847-56.
57. Valadi, H., et al., *Exosome-mediated transfer of mRNAs and microRNAs is a novel mechanism of genetic exchange between cells.* Nat Cell Biol, 2007. **9**(6): p. 654-9.
58. Hoog, J.L. and J. Lotvall, *Diversity of extracellular vesicles in human ejaculates revealed by cryo-electron microscopy.* J Extracell Vesicles, 2015. **4**: p. 28680.
59. Kowal, J., et al., *Proteomic comparison defines novel markers to characterize heterogeneous populations of extracellular vesicle subtypes.* Proc Natl Acad Sci U S A, 2016. **113**(8): p. E968-77.
60. Keerthikumar, S., et al., *Proteogenomic analysis reveals exosomes are more oncogenic than ectosomes.* Oncotarget, 2015. **6**(17): p. 15375-96.
61. Kalra, H., G.P. Drummen, and S. Mathivanan, *Focus on Extracellular Vesicles: Introducing the Next Small Big Thing.* Int J Mol Sci, 2016. **17**(2): p. 170.
62. Fruhbeis, C., et al., *Oligodendrocytes support axonal transport and maintenance via exosome secretion.* PLoS Biol, 2020. **18**(12): p. e3000621.
63. Faure, J., et al., *Exosomes are released by cultured cortical neurones.* Mol Cell Neurosci, 2006. **31**(4): p. 642-8.
64. Potolicchio, I., et al., *Proteomic analysis of microglia-derived exosomes: metabolic role of the aminopeptidase CD13 in neuropeptide catabolism.* J Immunol, 2005. **175**(4): p. 2237-43.
65. Taylor, A.R., et al., *Regulation of heat shock protein 70 release in astrocytes: role of signaling kinases.* Dev Neurobiol, 2007. **67**(13): p. 1815-29.
66. Lachenal, G., et al., *Release of exosomes from differentiated neurons and its regulation by synaptic glutamatergic activity.* Mol Cell Neurosci, 2011. **46**(2): p. 409-18.
67. Xu, B., et al., *Neurons secrete miR-132-containing exosomes to regulate brain vascular integrity.* Cell Res, 2017. **27**(7): p. 882-897.
68. Chivet, M., et al., *Exosomes secreted by cortical neurons upon glutamatergic synapse activation specifically interact with neurons.* J Extracell Vesicles, 2014. **3**: p. 24722.
69. Chivet, M., et al., *Exosomes as a novel way of interneuronal communication.* Biochem Soc Trans, 2013. **41**(1): p. 241-4.
70. Yang, Y., et al., *Epigenetic regulation of neuron-dependent induction of astroglial synaptic protein GLT1.* Glia, 2010. **58**(3): p. 277-86.
71. Men, Y., et al., *Exosome reporter mice reveal the involvement of exosomes in mediating neuron to astroglia communication in the CNS.* Nat Commun, 2019. **10**(1): p. 4136.
72. Bahrini, I., et al., *Neuronal exosomes facilitate synaptic pruning by up-regulating complement factors in microglia.* Sci Rep, 2015. **5**: p. 7989.
73. Fruhbeis, C., et al., *Extracellular vesicles as mediators of neuron-glia communication.* Front Cell Neurosci, 2013. **7**: p. 182.

74. Venturini, A., et al., *Exosomes From Astrocyte Processes: Signaling to Neurons.* Front Pharmacol, 2019. **10**: p. 1452.
75. Pascua-Maestro, R., et al., *Extracellular Vesicles Secreted by Astroglial Cells Transport Apolipoprotein D to Neurons and Mediate Neuronal Survival Upon Oxidative Stress.* Front Cell Neurosci, 2018. **12**: p. 526.
76. Mavroeidi, P., et al., *Exosomes in Alpha-Synucleinopathies: Propagators of Pathology or Potential Candidates for Nanotherapeutics?* Biomolecules, 2022. **12**(7).
77. Alvarez-Erviti, L., et al., *Delivery of siRNA to the mouse brain by systemic injection of targeted exosomes.* Nat Biotechnol, 2011. **29**(4): p. 341-5.
78. Grey, M., et al., *Acceleration of alpha-synuclein aggregation by exosomes.* J Biol Chem, 2015. **290**(5): p. 2969-82.
79. Poehler, A.M., et al., *Autophagy modulates SNCA/alpha-synuclein release, thereby generating a hostile microenvironment.* Autophagy, 2014. **10**(12): p. 2171-92.
80. Gustafsson, G., et al., *Secretion and Uptake of alpha-Synuclein Via Extracellular Vesicles in Cultured Cells.* Cell Mol Neurobiol, 2018. **38**(8): p. 1539-1550.
81. Zhang, S., et al., *Intercellular transfer of pathogenic alpha-synuclein by extracellular vesicles is induced by the lipid peroxidation product 4-hydroxynonenal.* Neurobiol Aging, 2018. **61**: p. 52-65.
82. Richter-Landsberg, C. and M. Heinrich, *OLN-93: a new permanent oligodendroglia cell line derived from primary rat brain glial cultures.* J Neurosci Res, 1996. **45**(2): p. 161-73.
83. Reimer, L., et al., *Inflammation kinase PKR phosphorylates alpha-synuclein and causes alpha-synuclein-dependent cell death.* Neurobiol Dis, 2018. **115**: p. 17-28.
84. Strohaker, T., et al., *Structural heterogeneity of alpha-synuclein fibrils amplified from patient brain extracts.* Nat Commun, 2019. **10**(1): p. 5535.
85. Thery, C., et al., *Isolation and characterization of exosomes from cell culture supernatants and biological fluids.* Curr Protoc Cell Biol, 2006. **Chapter 3**: p. Unit 3 22.
86. Ellman, G.L., et al., *A new and rapid colorimetric determination of acetylcholinesterase activity.* Biochem Pharmacol, 1961. **7**: p. 88-95.
87. An, K., et al., *Exosomes neutralize synaptic-plasticity-disrupting activity of Abeta assemblies in vivo.* Mol Brain, 2013. **6**: p. 47.
88. Tarutani, A., et al., *The Effect of Fragmented Pathogenic alpha-Synuclein Seeds on Prion-like Propagation.* J Biol Chem, 2016. **291**(36): p. 18675-88.
89. Prusiner, S.B., *Shattuck lecture--neurodegenerative diseases and prions.* N Engl J Med, 2001. **344**(20): p. 1516-26.
90. Bernis, M.E., et al., *Prion-like propagation of human brain-derived alpha-synuclein in transgenic mice expressing human wild-type alpha-synuclein.* Acta Neuropathol Commun, 2015. **3**: p. 75.
91. Melki, R., *Role of Different Alpha-Synuclein Strains in Synucleinopathies, Similarities with other Neurodegenerative Diseases.* J Parkinsons Dis, 2015. **5**(2): p. 217-27.
92. Bousset, L., et al., *Structural and functional characterization of two alpha-synuclein strains.* Nat Commun, 2013. **4**: p. 2575.
93. Peng, C., R.J. Gathagan, and V.M. Lee, *Distinct alpha-Synuclein strains and implications for heterogeneity among alpha-Synucleinopathies.* Neurobiol Dis, 2018. **109**(Pt B): p. 209-218.
94. Guerrero-Ferreira, R., et al., *New insights on the structure of alpha-synuclein fibrils using cryo-electron microscopy.* Curr Opin Neurobiol, 2020. **61**: p. 89-95.
95. Peng, C., et al., *Cellular milieu imparts distinct pathological alpha-synuclein strains in alpha-synucleinopathies.* Nature, 2018. **557**(7706): p. 558-563.
96. Van der Perren, A., et al., *The structural differences between patient-derived alpha-synuclein strains dictate characteristics of Parkinson's disease, multiple system atrophy and dementia with Lewy bodies.* Acta Neuropathol, 2020. **139**(6): p. 977-1000.

97. Lau, A., et al., *alpha-Synuclein strains target distinct brain regions and cell types.* Nat Neurosci, 2020. **23**(1): p. 21-31.
98. Shahnawaz, M., et al., *Discriminating alpha-synuclein strains in Parkinson's disease and multiple system atrophy.* Nature, 2020. **578**(7794): p. 273-277.
99. Woerman, A.L., et al., *MSA prions exhibit remarkable stability and resistance to inactivation.* Acta Neuropathol, 2018. **135**(1): p. 49-63.
100. Rey, N.L., et al., *Widespread transneuronal propagation of alpha-synucleinopathy triggered in olfactory bulb mimics prodromal Parkinson's disease.* J Exp Med, 2016. **213**(9): p. 1759-78.
101. Karampetsou, M., et al., *Phosphorylated exogenous alpha-synuclein fibrils exacerbate pathology and induce neuronal dysfunction in mice.* Sci Rep, 2017. **7**(1): p. 16533.
102. El-Agnaf, O.M., et al., *Alpha-synuclein implicated in Parkinson's disease is present in extracellular biological fluids, including human plasma.* FASEB J, 2003. **17**(13): p. 1945-7.
103. Guo, M., et al., *Microglial exosomes facilitate alpha-synuclein transmission in Parkinson's disease.* Brain, 2020. **143**(5): p. 1476-1497.
104. Stuendl, A., et al., *Induction of alpha-synuclein aggregate formation by CSF exosomes from patients with Parkinson's disease and dementia with Lewy bodies.* Brain, 2016. **139**(Pt 2): p. 481-94.
105. Devic, I., et al., *Salivary alpha-synuclein and DJ-1: potential biomarkers for Parkinson's disease.* Brain, 2011. **134**(Pt 7): p. e178.
106. Mollenhauer, B., et al., *Direct quantification of CSF alpha-synuclein by ELISA and first cross-sectional study in patients with neurodegeneration.* Exp Neurol, 2008. **213**(2): p. 315-25.
107. Wang, X., et al., *Detection of alpha-synuclein oligomers in red blood cells as a potential biomarker of Parkinson's disease.* Neurosci Lett, 2015. **599**: p. 115-9.
108. Llorens, F., et al., *Cerebrospinal alpha-synuclein in alpha-synuclein aggregation disorders: tau/alpha-synuclein ratio as potential biomarker for dementia with Lewy bodies.* J Neurol, 2016. **263**(11): p. 2271-2277.
109. Shahnawaz, M., et al., *Development of a Biochemical Diagnosis of Parkinson Disease by Detection of alpha-Synuclein Misfolded Aggregates in Cerebrospinal Fluid.* JAMA Neurol, 2017. **74**(2): p. 163-172.
110. Simonsen, A.H., et al., *The utility of alpha-synuclein as biofluid marker in neurodegenerative diseases: a systematic review of the literature.* Biomark Med, 2016. **10**(1): p. 19-34.
111. Chen, L. and M.B. Feany, *Alpha-synuclein phosphorylation controls neurotoxicity and inclusion formation in a Drosophila model of Parkinson disease.* Nat Neurosci, 2005. **8**(5): p. 657-63.
112. Smith, W.W., et al., *Alpha-synuclein phosphorylation enhances eosinophilic cytoplasmic inclusion formation in SH-SY5Y cells.* J Neurosci, 2005. **25**(23): p. 5544-52.
113. Sugeno, N., et al., *Serine 129 phosphorylation of alpha-synuclein induces unfolded protein response-mediated cell death.* J Biol Chem, 2008. **283**(34): p. 23179-88.
114. Azeredo da Silveira, S., et al., *Phosphorylation does not prompt, nor prevent, the formation of alpha-synuclein toxic species in a rat model of Parkinson's disease.* Hum Mol Genet, 2009. **18**(5): p. 872-87.
115. Mbefo, M.K., et al., *Phosphorylation of synucleins by members of the Polo-like kinase family.* J Biol Chem, 2010. **285**(4): p. 2807-22.
116. Chen, L., et al., *Tyrosine and serine phosphorylation of alpha-synuclein have opposing effects on neurotoxicity and soluble oligomer formation.* J Clin Invest, 2009. **119**(11): p. 3257-65.
117. Sato, H., et al., *Authentically phosphorylated alpha-synuclein at Ser129 accelerates neurodegeneration in a rat model of familial Parkinson's disease.* J Neurosci, 2011. **31**(46): p. 16884-94.

118. Ma, M.R., et al., *Phosphorylation induces distinct alpha-synuclein strain formation.* Sci Rep, 2016. **6**: p. 37130.
119. Anderson, J.P., et al., *Phosphorylation of Ser-129 is the dominant pathological modification of alpha-synuclein in familial and sporadic Lewy body disease.* J Biol Chem, 2006. **281**(40): p. 29739-52.
120. Fujiwara, H., et al., *alpha-Synuclein is phosphorylated in synucleinopathy lesions.* Nat Cell Biol, 2002. **4**(2): p. 160-4.
121. Sato, H., T. Kato, and S. Arawaka, *The role of Ser129 phosphorylation of alpha-synuclein in neurodegeneration of Parkinson's disease: a review of in vivo models.* Rev Neurosci, 2013. **24**(2): p. 115-23.
122. Walker, D.G., et al., *Changes in properties of serine 129 phosphorylated alpha-synuclein with progression of Lewy-type histopathology in human brains.* Exp Neurol, 2013. **240**: p. 190-204.
123. Giasson, B.I., et al., *Oxidative damage linked to neurodegeneration by selective alpha-synuclein nitration in synucleinopathy lesions.* Science, 2000. **290**(5493): p. 985-9.
124. Yu, Z., et al., *Nitrated alpha-synuclein induces the loss of dopaminergic neurons in the substantia nigra of rats.* PLoS One, 2010. **5**(4): p. e9956.
125. McCormack, A.L., S.K. Mak, and D.A. Di Monte, *Increased alpha-synuclein phosphorylation and nitration in the aging primate substantia nigra.* Cell Death Dis, 2012. **3**: p. e315.
126. Souza, J.M., G. Peluffo, and R. Radi, *Protein tyrosine nitration--functional alteration or just a biomarker?* Free Radic Biol Med, 2008. **45**(4): p. 357-66.
127. Sorrentino, Z.A. and B.I. Giasson, *The emerging role of alpha-synuclein truncation in aggregation and disease.* J Biol Chem, 2020. **295**(30): p. 10224-10244.
128. Kellie, J.F., et al., *Quantitative measurement of intact alpha-synuclein proteoforms from post-mortem control and Parkinson's disease brain tissue by intact protein mass spectrometry.* Sci Rep, 2014. **4**: p. 5797.
129. Li, W., et al., *Aggregation promoting C-terminal truncation of alpha-synuclein is a normal cellular process and is enhanced by the familial Parkinson's disease-linked mutations.* Proc Natl Acad Sci U S A, 2005. **102**(6): p. 2162-7.
130. Liu, C.W., et al., *A precipitating role for truncated alpha-synuclein and the proteasome in alpha-synuclein aggregation: implications for pathogenesis of Parkinson disease.* J Biol Chem, 2005. **280**(24): p. 22670-8.
131. Baba, M., et al., *Aggregation of alpha-synuclein in Lewy bodies of sporadic Parkinson's disease and dementia with Lewy bodies.* Am J Pathol, 1998. **152**(4): p. 879-84.
132. Lee, M.K., et al., *Human alpha-synuclein-harboring familial Parkinson's disease-linked Ala-53 --> Thr mutation causes neurodegenerative disease with alpha-synuclein aggregation in transgenic mice.* Proc Natl Acad Sci U S A, 2002. **99**(13): p. 8968-73.
133. Zhang, Z., et al., *Asparagine endopeptidase cleaves alpha-synuclein and mediates pathologic activities in Parkinson's disease.* Nat Struct Mol Biol, 2017. **24**(8): p. 632-642.
134. Sorrentino, Z.A., et al., *Physiological C-terminal truncation of alpha-synuclein potentiates the prion-like formation of pathological inclusions.* J Biol Chem, 2018. **293**(49): p. 18914-18932.
135. Murray, I.V., et al., *Role of alpha-synuclein carboxy-terminus on fibril formation in vitro.* Biochemistry, 2003. **42**(28): p. 8530-40.
136. Serpell, L.C., et al., *Fiber diffraction of synthetic alpha-synuclein filaments shows amyloid-like cross-beta conformation.* Proc Natl Acad Sci U S A, 2000. **97**(9): p. 4897-902.
137. Levin, J., et al., *Increased alpha-synuclein aggregation following limited cleavage by certain matrix metalloproteinases.* Exp Neurol, 2009. **215**(1): p. 201-8.
138. van der Wateren, I.M., et al., *C-terminal truncation of alpha-synuclein promotes amyloid fibril amplification at physiological pH.* Chem Sci, 2018. **9**(25): p. 5506-5516.

139. Wang, W., et al., *Caspase-1 causes truncation and aggregation of the Parkinson's disease-associated protein alpha-synuclein.* Proc Natl Acad Sci U S A, 2016. **113**(34): p. 9587-92.
140. Ma, L., et al., *C-terminal truncation exacerbates the aggregation and cytotoxicity of alpha-Synuclein: A vicious cycle in Parkinson's disease.* Biochim Biophys Acta Mol Basis Dis, 2018. **1864**(12): p. 3714-3725.
141. Sorrentino, Z.A., et al., *Carboxy-terminal truncations of mouse alpha-synuclein alter aggregation and prion-like seeding.* FEBS Lett, 2020. **594**(8): p. 1271-1283.
142. Levitan, K., et al., *Conserved C-terminal charge exerts a profound influence on the aggregation rate of alpha-synuclein.* J Mol Biol, 2011. **411**(2): p. 329-33.
143. McGlinchey, R.P., et al., *C-terminal alpha-synuclein truncations are linked to cysteine cathepsin activity in Parkinson's disease.* J Biol Chem, 2019. **294**(25): p. 9973-9984.
144. Karpowicz, R.J., Jr., J.Q. Trojanowski, and V.M. Lee, *Transmission of alpha-synuclein seeds in neurodegenerative disease: recent developments.* Lab Invest, 2019. **99**(7): p. 971-981.
145. Pieri, L., et al., *Cellular response of human neuroblastoma cells to alpha-synuclein fibrils, the main constituent of Lewy bodies.* Biochim Biophys Acta, 2016. **1860**(1 Pt A): p. 8-19.
146. Cuervo, A.M., et al., *Impaired degradation of mutant alpha-synuclein by chaperone-mediated autophagy.* Science, 2004. **305**(5688): p. 1292-5.
147. Stefanis, L., et al., *How is alpha-synuclein cleared from the cell?* J Neurochem, 2019. **150**(5): p. 577-590.
148. McGlinchey, R.P. and J.C. Lee, *Cysteine cathepsins are essential in lysosomal degradation of alpha-synuclein.* Proc Natl Acad Sci U S A, 2015. **112**(30): p. 9322-7.
149. Bennett, M.C., et al., *Degradation of alpha-synuclein by proteasome.* J Biol Chem, 1999. **274**(48): p. 33855-8.
150. Iwata, A., et al., *Alpha-synuclein degradation by serine protease neurosin: implication for pathogenesis of synucleinopathies.* Hum Mol Genet, 2003. **12**(20): p. 2625-35.
151. Dufty, B.M., et al., *Calpain-cleavage of alpha-synuclein: connecting proteolytic processing to disease-linked aggregation.* Am J Pathol, 2007. **170**(5): p. 1725-38.
152. Dickson, D.W., et al., *Widespread alterations of alpha-synuclein in multiple system atrophy.* Am J Pathol, 1999. **155**(4): p. 1241-51.
153. Mavroeidi, P., et al., *Autophagy mediates the clearance of oligodendroglial SNCA/alpha-synuclein and TPPP/p25A in multiple system atrophy models.* Autophagy, 2022. **18**(9): p. 2104-2133.
154. Lehotzky, A., et al., *Zinc-induced structural changes of the disordered tppp/p25 inhibits its degradation by the proteasome.* Biochim Biophys Acta, 2015. **1852**(1): p. 83-91.